Soil moisture-atmosphere coupling strength over Central Europe in the recent warming climate

Thomas Schwitalla[1], Lisa Jach[1], Volker Wulfmeyer[1], Kirsten Warrach-Sagi[1]

[1]Institute of Physics and Meteorology, University of Hohenheim, Garbenstrasse 30, 70599 Stuttgart, Germany

Correspondence to: Thomas Schwitalla (Thomas.Schwitalla@uni-hohenheim.de)

Abstract

In the last decades, Europe more often experiences periods of severe drought and heatwaves which have a major impact on agriculture and society. While land surface conditions were found to be crucial for exacerbating duration and intensity of these events, their influence is typically quantified for climate periods or single events. To provide an overview of how surface conditions shape land-atmosphere (LA) coupling, this study investigates interannual variability of LA coupling strength. The focus is set on the warm and dry summer seasons 2003-2022 over Central Europe and the ERA5 data set is applied.

Especially the drought summer seasons 2003, 2018, and 2022 can be identified by the changing soil moisture-atmosphere coupling pattern in turn leading to an increased lifted condensation level height inhibiting local deep convection triggering. Summer 2021 was a special case as spring precipitation was on average and a heavy rain event occurred during July, resulting in high moisture availability leading to a change in the LA feedback strength. During the warm and wet summers 1997 and 2002 no strong soil moisture-atmosphere coupling is observed as there is always enough soil moisture available for evaporation. The results obtained with respect to LA coupling strength reflect a shift in the coupling relationships toward reinforced heating and drying by the land surface under heatwave and drought conditions, whose frequency is increasing with ongoing climate change.

1 Introduction

In the last decades, Europe experienced severe drought periods and heatwaves (WMO, 2015; C3S, 2018; Markonis et al., 2021; WMO, 2022a) where 2022 was the hottest summer ever recorded over Europe (WMO, 2022a). Precipitation exhibited a strong dry anomaly during summer over Central Europe in 2003, 2018 and 2022 (WMO, 2004, 2018; C3S, 2018; WMO, 2022b; Spensberger et al., 2020). At the same time, the soil experienced an exceptional dryness in the uppermost 25 cm (Boeing et al., 2022; Rakovec et al., 2022) as shown by the soil moisture index developed by Zink et al. (2016). This was also shown by Rousi et al. (2023) and Dirmeyer et al. (2021) for 2018, who suggest that these extreme conditions will be more likely under climate change conditions where two out of three summer seasons will experience hot and dry conditions. Rousi et al. (2022) identified Europe as a heatwave hot spot where heat waves are three to four times more likely than in other areas of the midlatitudes due to the occurrence of double-jet stream situations (Kornhuber et al., 2017).

Land-atmosphere (LA) coupling generally describes the co-variability of atmospheric conditions (e.g., planetary boundary layer (PBL) height, convective available potential energy (CAPE), lifted condensation level (LCL)) and the condition of the land surface (e.g., vegetation, soil moisture) (Findell and Eltahir, 2003b; Koster et al., 2004; Dirmeyer, 2011; Guo et al., 2006). In the context of extremes, it was identified as a driver and intensifier for the duration and intensity of heat waves and droughts (van Heerwaarden and Teuling, 2014; Ukkola et al., 2018;

Schumacher et al., 2022). Miralles et al. (2019) and Schumacher et al. (2022) showed the existence of a self-propagating mechanism of droughts. Meteorological droughts intensify due to increased water vapor deficit (VPD) inside the PBL which feeds back into an intensified depletion of surface moisture reservoirs.

One of these reservoirs is soil moisture, which plays a key role for the climate due to its influence on the partitioning between surface sensible and latent heat fluxes of the incoming solar energy (Seneviratne et al., 2010; Stephens et al., 2023). In vegetated areas the surface latent heat flux additionally depends on the atmospheric water vapor deficit (VPD), air temperature, incoming radiation, and vegetation properties (stomatal resistance, leaf area index (LAI) and rooting depth) (Miralles et al., 2019; Warrach-Sagi et al., 2022). In consequence of spatial and temporal variability in these influencing factors, LA feedback often shows regional, but also temporal variations, especially under climate change conditions (Seneviratne et al., 2006; Denissen et al., 2022; Jach et al., 2022).

Knist et al. (2017) investigated the long-term average relationship between root zone soil moisture and surface fluxes by means of different regional climate model (RCM) simulations for the period 1989-2008 for the European summer seasons. They identified a coupling hot spot region for the surface coupling of sensible and latent heat fluxes and latent heat flux and 2-m temperature in South Europe while a transition zone is present over larger parts of Central Europe. Jach et al. (2022) performed a RCM LA coupling sensitivity experiment with respect to climate change signals of temperature and humidity for the period 1986-2015. Their results revealed a permanent coupling hot spot over Northeast and East Europe with the location being insensitive to changes in low level moisture and temperature. While there was only little sensitivity over the northern part of this area, Central Europe and the British Isles showed change in the coupling regime based on the CTP-HI_{low} framework (Findell and Eltahir, 2003a, 2003b). Warrach-Sagi et al. (2022) evaluated the atmospheric coupling index (ACI; Guo et al., 2006; Dirmeyer, 2011) using an RCM and found a strong sensitivity between sensible heat flux and CAPE during the growing season 2005 over South Germany which is complemented by a study of Leutwyler et al. (2021) who found a strong soil moisture – precipitation feedback over Central Europe during the summer seasons 1999-2008.

Several studies investigated the relation of soil moisture with recent European heat waves and droughts. Hauser et al. (2016) found that a soil moisture-temperature feedback was, among a wave train (Di Capua et al., 2021), a key driver for the severe heat wave over Siberia in 2010, while Dirmeyer et al. (2021) and Orth (2021) found that it was a key driver for the European heatwave in 2018. García-Herrera et al. (2010) found that a strong soil moisture deficit was also one of the key drivers for the 2003 European heat wave. The study of Miralles et al. (2014) suggests that the heatwaves over Europe in 2003 and over Russia in 2010 were enhanced by a persistent large scale weather pattern associated with a strong soil moisture decay. The analysis of Dirmeyer et al. (2021) for the 2018 European heatwave revealed enhanced soil moisture – near-surface feedback under drought conditions. The exceptionally low soil moisture limited evapotranspiration and thus amplified the heat wave due to reduced evaporative cooling (Santanello et al., 2018).This led to one of the most severe heatwaves over Europe since 1979 (Becker et al., 2022). Wehrli et al. (2019) found that soil moisture and the large scale weather pattern are equally important for the duration and intensity of heatwaves around the globe. According to Ossó et al. (2022), Europe already faced an increase in climate extremes since 2000 and will remain a hot spot for severe droughts (Huebener et al., 2017; van der Wiel et al., 2022) impacting not only summer's crop yields (Toreti et al., 2022) but also affecting the generation of renewable energy.

The in the preceding paragraph described shifts in the hydrological conditions from energy- to moisture-limited conditions originating from droughts and heatwaves (Dirmeyer et al., 2021; Duan et al., 2020) or severe flooding (Lo et al., 2021) imply temporal variability in LA coupling at sub-seasonal to interannual time-scales. Guo and

Dirmeyer (2013) also found interannual variability in soil moisture-precipitation coupling in consequence of different soil moisture availability. Additionally, the critical soil moisture thresholds (Dirmeyer et al., 2021; Rousi et al., 2023) suggest not only an intensification of the heat and drought conditions by LA coupling over Europe but also a strengthening of the coupling itself. However, a quantification of temporal variability in different coupling relationships, as well as understanding of the impact of the variability remain lacking, as LA coupling strength was barely investigated over Europe, and particularly on other time scales than climate periods, so far. The same applies to shifts between coupling regimes due to variability in the climatic conditions.

In this study, we therefore assess the temporal variability of LA coupling of the European summer seasons 1991-2022 on the interannual time scale in dependence on temperature, soil moisture, precipitation and large-scale weather pattern by applying data from the fifth generation European Centre for Medium Range Weather Forecasting (ECMWF) atmospheric reanalysis (ERA5; Hersbach et al., 2020) and the ENSEMBLES daily gridded observational dataset for precipitation (E-OBS; Cornes et al., 2018).

The paper is structured as follows: Section 2 describes the applied data sets, selected coupling indices and the classification of the summer seasons . Section 3 describes the large-scale weather pattern and anomalies of 500 hPa geopotential, 2-m temperatures, precipitation, and soil moisture followed by the LA coupling analysis in section 4. Section 5 discusses our results. Finally, section 6 summarizes our work and provides an outlook on potential future research.

2 Material and Methods

2.1 Datasets

For the analysis of the LA feedback regions, the fifth generation European Centre for Medium Range Weather Forecasting (ECMWF) atmospheric reanalysis (ERA5; Hersbach et al., 2020) was used. ERA5 is produced by the Copernicus Climate Change Service (C3S, http://climate.copernicus.eu/) at ECMWF. This data set provides hourly estimates of atmospheric, surface, and oceanic variables on a horizontal resolution of ~ 30 km and includes the assimilation of observations. ERA5 clearly outperforms its predecessor ERA-Interim (Dee et al., 2011; Martens et al., 2020) and makes use of sophisticated atmospheric data assimilation including satellite derived soil moisture data (Albergel et al., 2012) to its land-surface model (LSM) HTESSEL (Balsamo et al., 2009).

ERA5 has been recently applied in LA feedback studies over Europe (Rousi et al., 2023; Rousi et al., 2022) and other regions (Sun et al., 2021; Qi et al., 2023). Other reanalysis data sets like UERRA, only available until 2019, are not recommended to use if surface fluxes are required for analysis (https://confluence.ecmwf.int/display/UER/Issues+with+data). COSMO-REA6 (Bollmeyer et al., 2015) is only available from 1995-2019 and does neither make use of a sophisticated data assimilation scheme nor of an ensemble approach. The Climate Forecast System Reanalysis (CFSR; Schneider et al., 2013) is only available until 2010 and thus does not cover the recent climate change period. To summarize, ERA5 data deliver the required 3D data to apply LA feedback metrics that combine the variables of our study.

Following the World Meteorological Organization's (WMO) recommendation to adjust the climate normal period (WMO, 2017), the summer seasons of 1991-2020 serve as reference period for the calculation of anomalies. The investigation period covers the summer seasons between 1991-2022 over an area between 5°W-25°E and 40°N-60°N (see Fig. 1). Reasons to choose very recent summers were, among others, that the first half of summer 2021 was very warm and dry while an extreme precipitation event (Mohr et al., 2023) led to a sudden increase in soil

moisture over France, Benelux, and West Germany. Summer 2022 was the hottest summer seasons ever recorded over Europe associated with a west-east soil moisture anomaly pattern (C3S, 2023). Overall, both recent summer seasons reflect the climate change trend over Europe.

To categorize the summer seasons during this period into warm and wet, warm and dry, and cold summer seasons, seasonal mean anomalies of ERA5 2-m temperatures and the ENSEMBLES daily gridded observational dataset for precipitation (E-OBS; Cornes et al., 2018) version V26.0e precipitation were calculated. To complement our analysis, seasonal mean anomalies of 500 hPa geopotential (Lhotka and Kyselý, 2022) and volumetric root zone soil moisture were calculated from ERA5. All anomalies were calculated using the Climate Data Operators (CDO) version 2.0.5 (Schulzweida, 2022).

2.2 LA coupling indices

In our study we apply the statistical LA feedback metrics, namely the terrestrial coupling index (TCI) and atmospheric coupling index (ACI), described in Guo et al. (2006), Dirmeyer (2011), and Santanello et al. (2018). To calculate the different indices, we used a combination of the NCAR Command Language (NCL, Brown et al., 2012) together with the FORTRAN programs provided by Tawfik (2015).

For our analysis, we used volumetric root zone soil moisture η, defined as weighted sum of the soil moisture in the top three soil layers of ERA5 down to 1 m below the surface, surface latent and sensible heat fluxes (LH and SH), CAPE, and PBL height (PBLH). In addition, we used the lifted condensation height (HLCL) and the lifted condensation height deficit (LCL deficit), defined as difference between HLCL and PBLH. As HLCL was not available from ERA5, we used the approach from Georgakakos and Bras (1984) and Bolton (1980) which is based on surface pressure, 2-m temperature, and 2-m dewpoint to derive HLCL which is also applied in Dirmeyer et al. (2014).

The strength of the TCI (Eq. 1) is defined as

$$TCI = \sigma(\eta)\frac{dLH}{d\eta} \quad (1)$$

where dLH/dη is the slope of the linear regression between the surface latent heat flux (LH) and the root zone soil moisture η as described in Santanello et al. (2018). A positive TCI describes the sensitivity of LH with respect to changes in the root zone soil moisture. To derive the strength of the coupling between the land surface and the atmosphere (ACI), soil moisture can, e.g., be substituted by surface fluxes in Eq. 1 while LH can be substituted by an atmospheric variable sensitive to LH changes such as the planetary boundary layer height, or CAPE (Dirmeyer et al., 2014).

The daily mean values are calculated between 06 UTC and 18 UTC (Yin et al., 2023) as e.g., the surface latent heat fluxes during night-time becomes close to zero with very little variations during this time. Also, during night-time, PBLH collapses to small values and stays often constant which has a detrimental impact on the LA-feedback analysis. Water grid cells are not considered in our evaluation.

2.3 Classification of summer seasons

For the classification of the summer seasons with respect to temperature (Table 1), we calculated the spatial median of the 2-m temperature anomalies from ERA5 with respect to the summer mean 1991-2020 over Europe. If the 2-

m temperature anomaly is larger than 0.5°C, the corresponding summer season is used for our analysis. For the classification only land grid cells between 40°N-60°N and 5°W-25°E were considered.

Year	2003	2006	2015	2017	2018	2019	2020	2021	2022
E-OBS Precipitation anomaly [mm]	-60.4	-0.4	-34.3	-9.3	-37.8	-34.7	7.8	-3.7	-63.0
ERA5 Precipitation anomaly [mm]	-59.4	-8.7	-38.9	0.2	-36.1	-32.4	17.0	15.1	-37.9

Table 1. Selected summer seasons based on a positive temperature anomaly larger than 0.5°C with respect to the climatological mean 1991-2020. As a reference, the median precipitation anomaly from E-OBS (2nd row) and ERA5 (3rd row) is given. Note the wet anomaly year 2020 is included though the median 2-m temperature anomaly for 2020 was only 0.45 °C but this was the only summer with a moderate positive precipitation bias in the last decade.

Although the median 2-m temperature anomaly for 2020 was only 0.45 °C, 2020 is considered in our analysis as this was the only summer with a moderate positive precipitation bias in the last decade. As shown in Table 1 the warm and dry summer seasons became the prevailing situation since 2015 associated with a strong reduction in annual and seasonal precipitation, combined with a reduced atmospheric water availability that led to a constant decline of the root zone soil moisture and thus an agricultural drought which was the case, e.g., in 2018-2020 over Europe (van der Wiel et al., 2022).

3 Summer season anomaly maps

The following sections describe the characteristics of the summer seasons chosen for evaluation (Table 1) with respect to ERA5 500 hPa geopotential, 2-m temperature root zone soil moisture η ,as well as observed and ERA5 simulated precipitation..

3.1 500 hPa geopotential

Figure 1 shows the 500 hPa geopotential height anomalies for the selected summer seasons. The 500 hPa geopotential height helps to determine mid-tropospheric troughs and ridges describing the large-scale weather pattern. The summer seasons are in general characterized by strong positive 500 hPa geopotential anomalies over major parts of Europe. However, summer 2015 and 2020 are exceptions. In 2015, a pronounced north-south anomaly gradient is visible with negative values over the British Isles and Scandinavia while in 2020 the 500 hPa geopotential is only slightly above the average 1991-2020 (bottom right panel in Fig. 1).

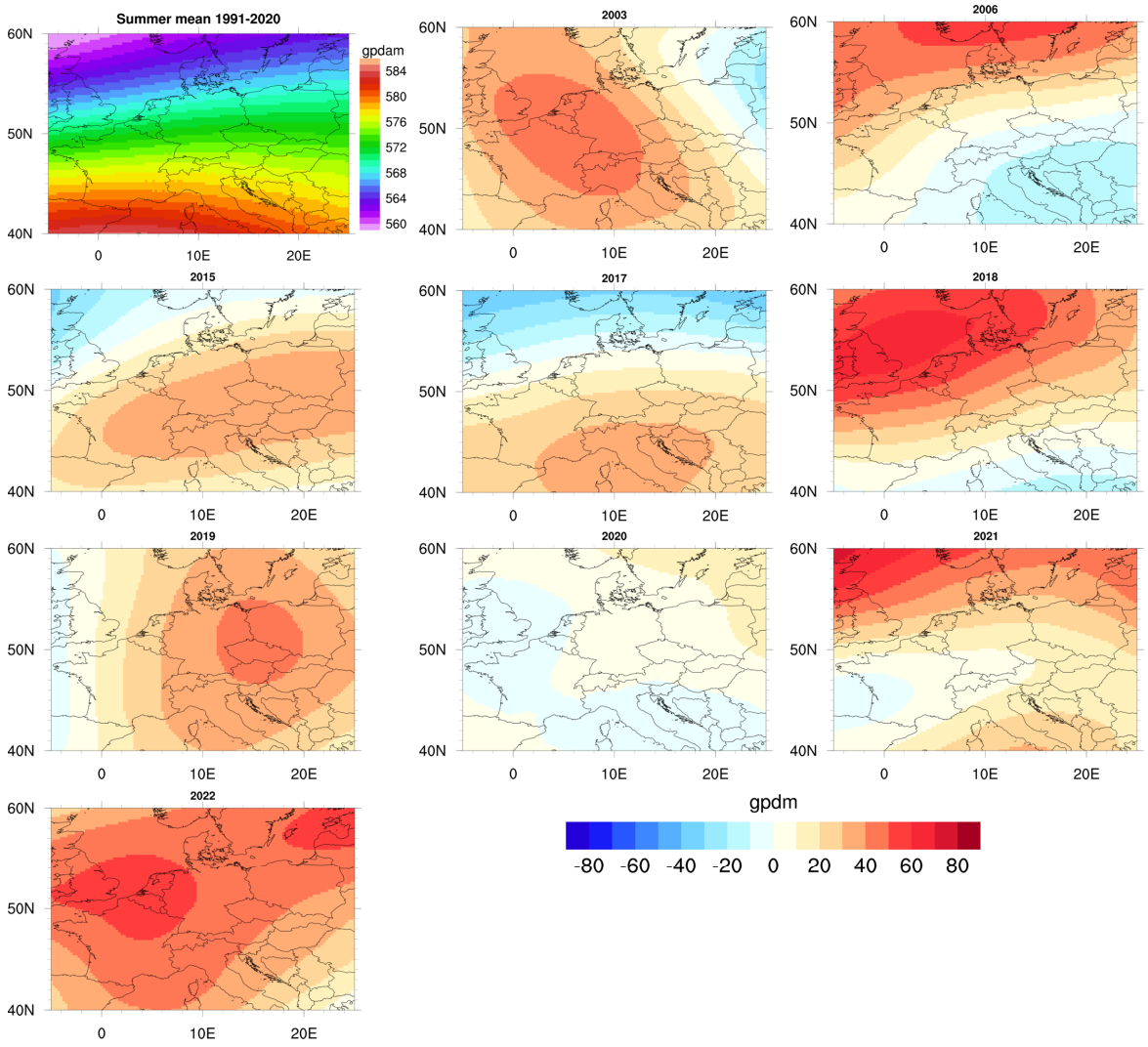

Figure 1. ERA5 500hPa geopotential anomalies for the selected summer seasons (Table 1). The top left panel shows the mean summer 500 hPa geopotential 1991-2020 from ERA5.

3.2 Surface temperature

The positive 500 hPa geopotential anomalies shown in Fig. 1 are generally associated with positive 2-m temperature anomalies. the highest 2-m temperature anomalies were present in 2003, 2018, 2019, and 2022 (Fig. 2) which is associated with strong positive geopotential anomalies over Central Europe. 2022 was the hottest summer ever recorded so far (C3S, 2023). During 2006, the 2-m temperature anomalies are highest north of 51°N while in 2017, the highest temperature anomalies were observed south of 50°N as the maximum geopotential anomaly is shifted to the north and south, respectively. Summer 2020 shows positive temperature anomalies over a wide area of our investigation domain, however the 500 hPa anomalies were very moderate pointing towards a constant flow of warm and moist airmasses towards Central Europe.

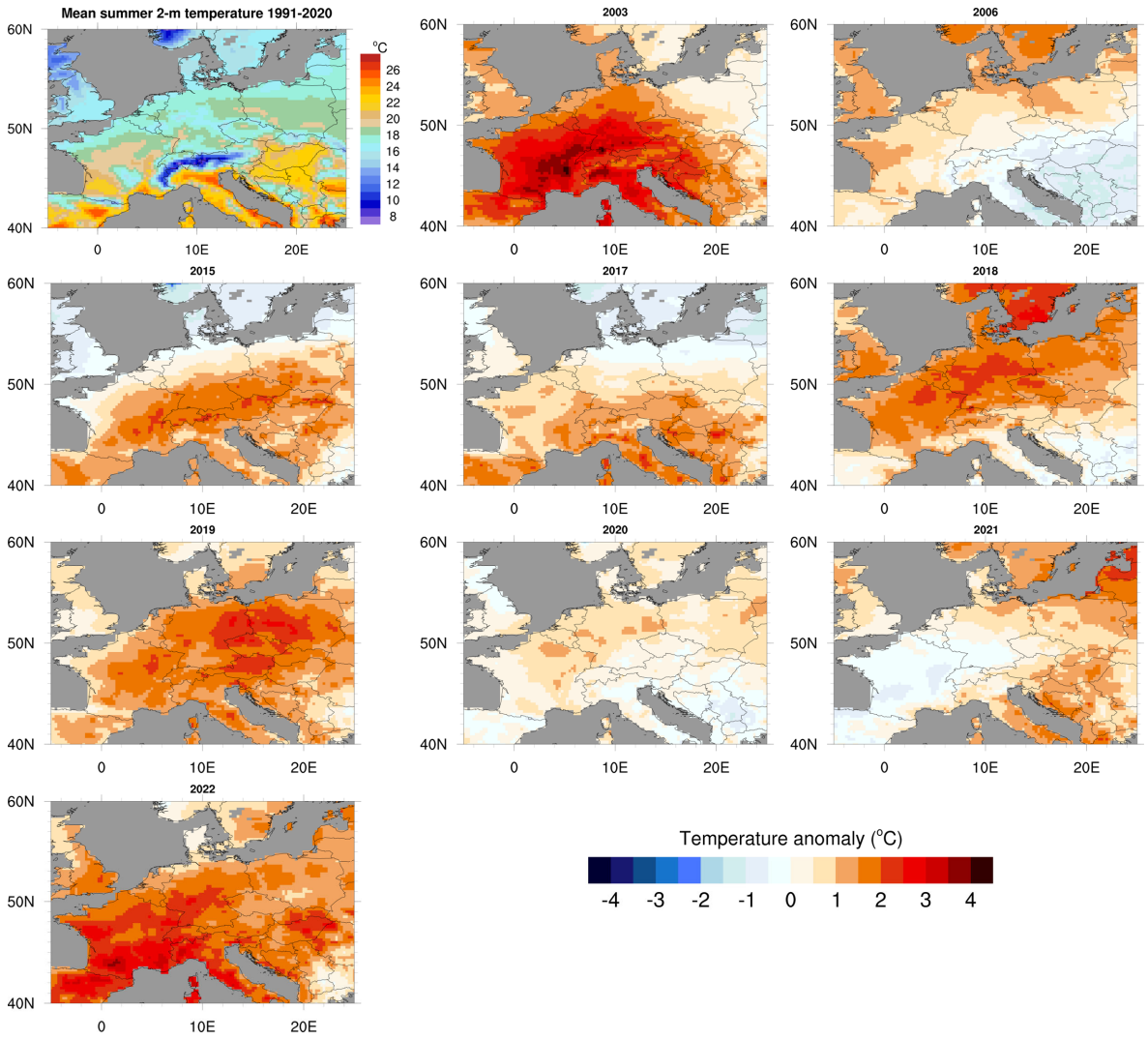

Figure 2. ERA5 2-m temperature anomalies. The top left panel shows the mean summer 2-m temperatures 1991-2020 from ERA5.

3.3 Precipitation

Observed Precipitation (Fig. 3 and Table 1) is often well below the climatological average 1991-2020except for 2006 and 2021. 2003, 2018, 2019 and 2022 were exceptionally dry (Rousi et al., 2023; Rousi et al., 2022) with a median precipitation anomaly between -34 and -63 mm. These extreme anomalies are also seen in the precipitation anomalies derived from ERA5 (Fig. 4) which reasonably catches these dry periods (Lavers et al., 2022). With respect to precipitation derived from E-OBS, 2006 can be seen as an average year with moderate precipitation anomalies over Central Europe. 2020 shows strong to moderate precipitation anomalies both in E-OBS and ERA5 over Germany, France, Poland, and Benelux while precipitation over Southeast Europe is above the climatological average resulting in a positive precipitation anomaly in both data sets. Although temperatures in 2021 were well above the climatological average 1991-2020, precipitation over France, Benelux, and Germany was above average due to a small scale low-pressure system which caused the Ahr flood event (Mohr et al., 2023) (Fig 3).This event was also simulated by ERA5 as indicated by the dark teal colors in Fig. 4. A statistical evaluation revealed correlations between -0.25 and -0.65 between precipitation and temperature during the summer seasons presented here indicating a precipitation dry bias in case of strong positive temperature anomalies.

3.4 Root zone soil moisture

Figure 5 displays the ERA5 derived root zone soil moisture anomalies. Here 2003, 2018, and 2022 show the lowest root zone soil moisture availability over Germany, Benelux and France. This relates to the strong positive temperature bias (sec. 3.2) and the precipitation dry bias shown both by E-OBS and ERA5 (sec. 3.1). Interestingly, although 2019 was also among of the warmest and driest summers, the soil moisture dry bias is less pronounced as in the other three years pointing towards a higher soil moisture content during spring (Fig. S2). 2021 shows strong positive soil moisture anomaly over Benelux and Germany which was related to colder than average April and May 2021 (C3S, 2022). By using the median of the soil moisture anomalies, 2006 largely is an average summer with moderate positive anomalies over East Europe while 2015 and 2017 on average show moderate dry soil anomalies.

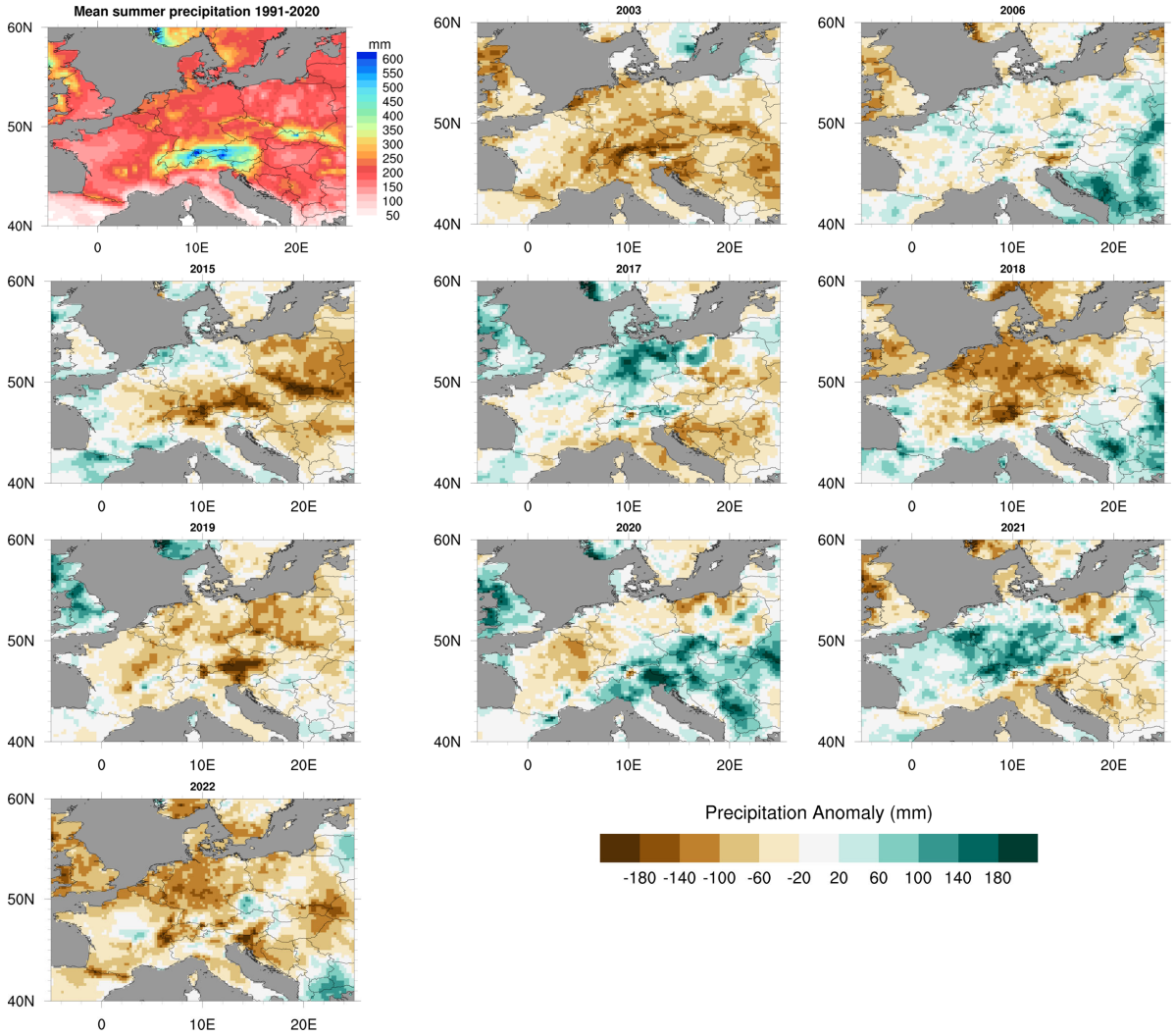

Figure 3. E-OBS precipitation anomalies for the selected summer seasons with respect to the mean summer precipitation 1991-2020 shown in the top left panel.

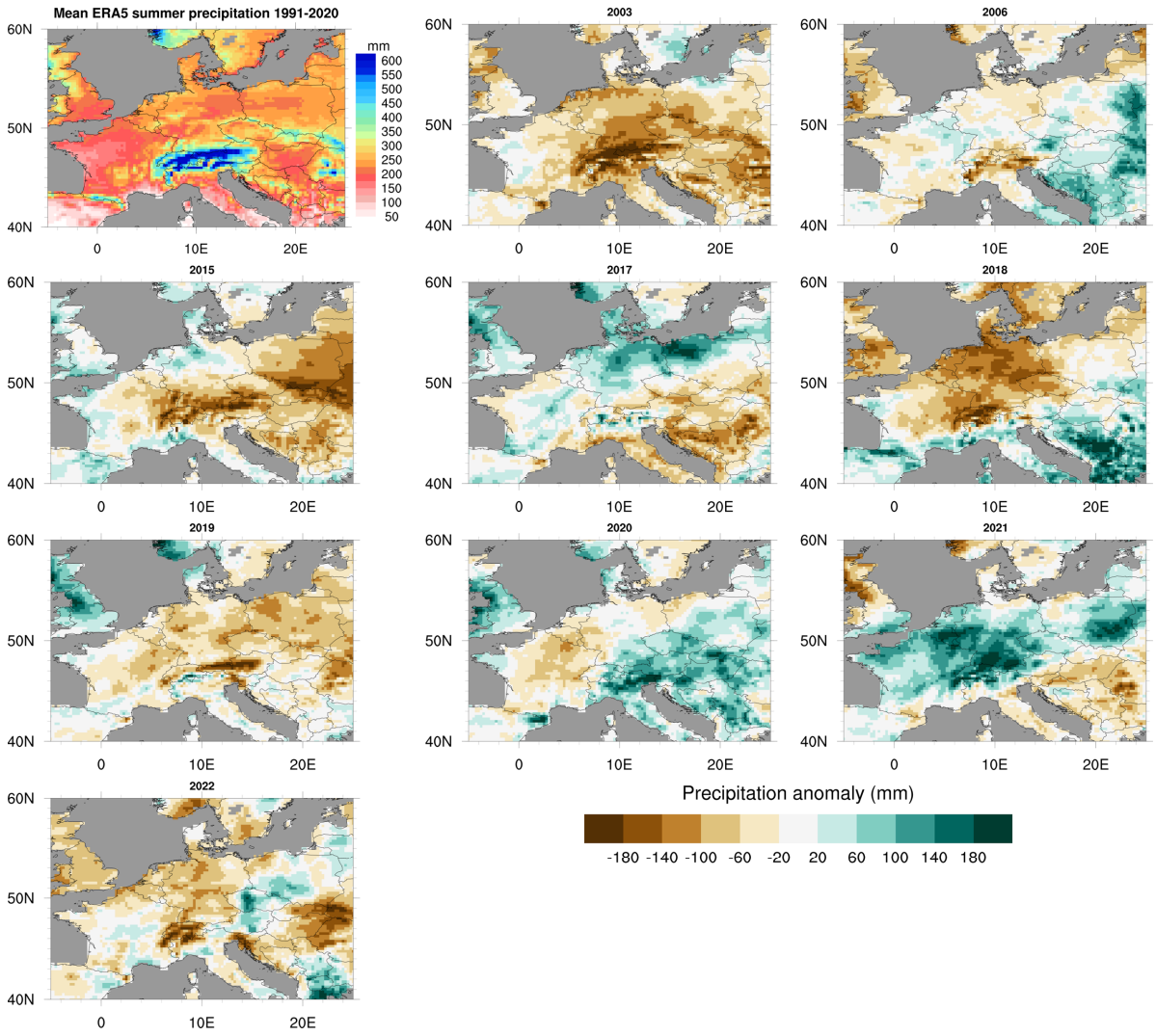

Figure 4. Same as Fig. 3 but for ERA5.

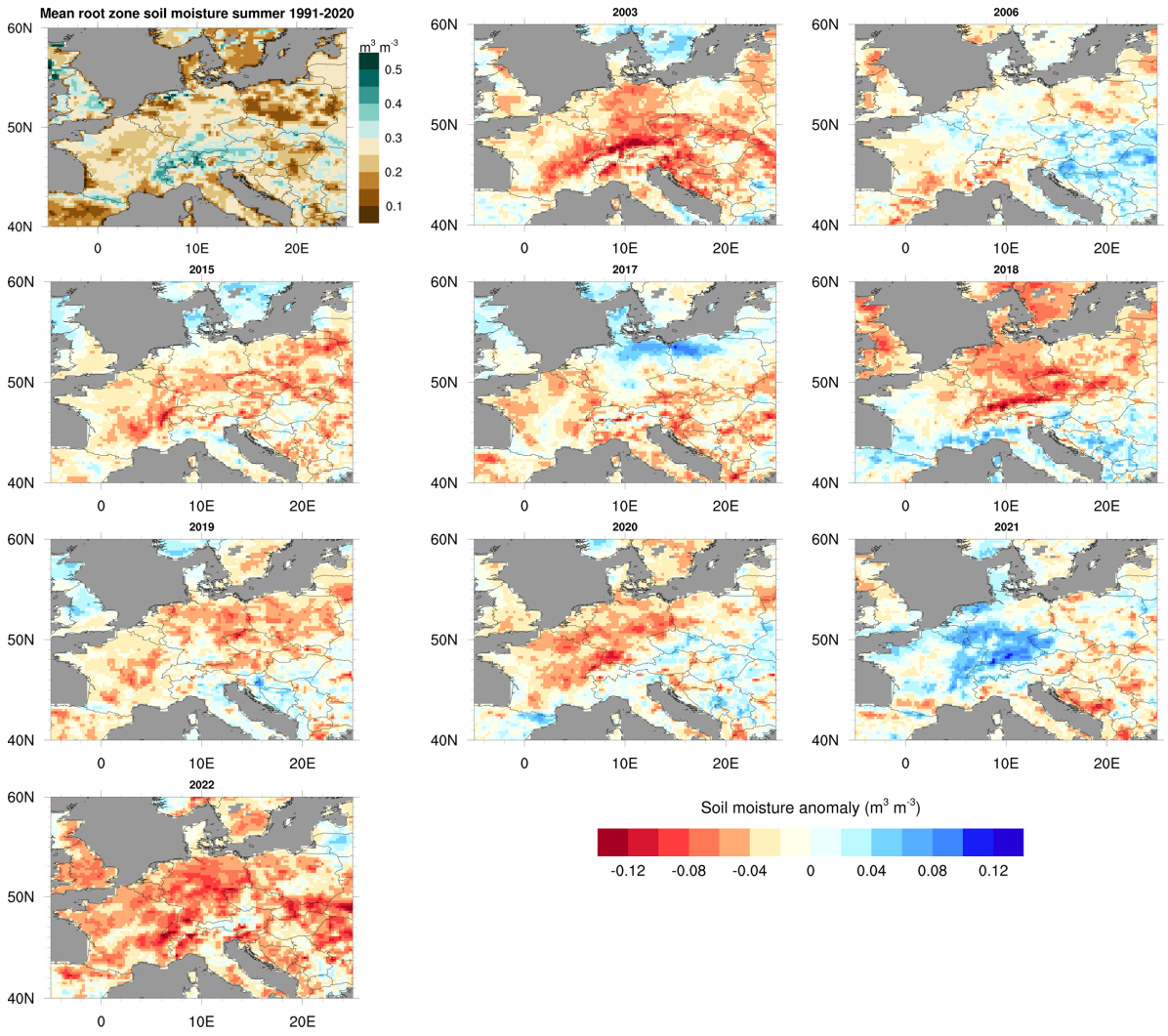

Figure 5. ERA5 root soil moisture anomalies with respect to the summer mean 1991-2020 (top left panel) for the selected summer seasons

220

225

4 Results

4.1 Terrestrial coupling strength

In this section, we will present the terrestrial coupling index following Dirmeyer (2011)for the selected summer seasons. As we are interested in daytime properties, we only used data between 06 UTC and 18 UTC to derive
230 daily mean values from ERA5. According to Findell et al. (2015), a 92 day period is sufficient for LA feedback analysis on individual data sets.

In addition, the Pearson correlation coefficient between surface sensible (SH) and latent heat flux (LH) is shown which can also be used as an indicator for LA coupling (Knist et al., 2017). Water grid cells are not considered for the analysis.

235 Fig. 6 shows the TCIs of the summer seasons categorized as warm and dry which became the dominant situation over Central Europe since 2015. The TCI between η and LH describes how changes in soil moisture drives variations in the surface latent heat flux. A positive TCI denotes that LH is limited by the root zone soil moisture and the soil moisture variation results in LH variation while a negative TCI indicates that the development of LH

is energy limited, i.e., the incoming energy determines the LH development. In case the absolute TCI is low, either there is too little soil moisture available for evaporation, close to the wilting point, or the soil is too wet and a further increase does not lead to considerable changes in evaporation (Müller et al., 2021). The very warm and dry seasons 2003, 2018, 2019 and 2022 show a strong positive TCI over the regions affected by low soil moisture (Germany, France, and Benelux; Fig. 5). During 2006, which is considered as an average summer with respect to temperature, soil moisture and precipitation, the TCI shows a heterogenous pattern with neutral to slightly positive values of up to 20 W m^{-2} over most parts of Central Europe. The only exception is the alpine area and the most far eastern part of our validation domain where the TCI is slightly negative. In 2015, which overall is a very dry year with respect to soil moisture and precipitation, shows neutral values over North Germany while the rest of the investigation domain shows positive values. During 2017, TCI over Germany shows neutral values as apparently enough soil moisture is available (Fig. 5) while it is mostly negative south of 48°N. During 2020, TCI shows a heterogenous pattern as a moderate NW-SE precipitation and soil moisture anomaly gradient is present while at the same time temperature anomalies are in the range of less than ± 1.5 K.

During 2021, when a positive η anomaly is observed over Germany, Benelux, eastern France (Fig. 5) (C3S, 2022), the TCI becomes moderately negative in these region with values of about -20 W m^{-2} (Fig. 6). Apparently this is related to an already moist spring season (Fig. S2) and the heavy precipitation event occurring in June 2021 (Mohr et al., 2023) leading to a soil moisture content close to field capacity (middle panel of Fig. S1). A similar behavior of the TCI is observed during the two cold and wet summer seasons 1997 and 2002 (Fig. S7).

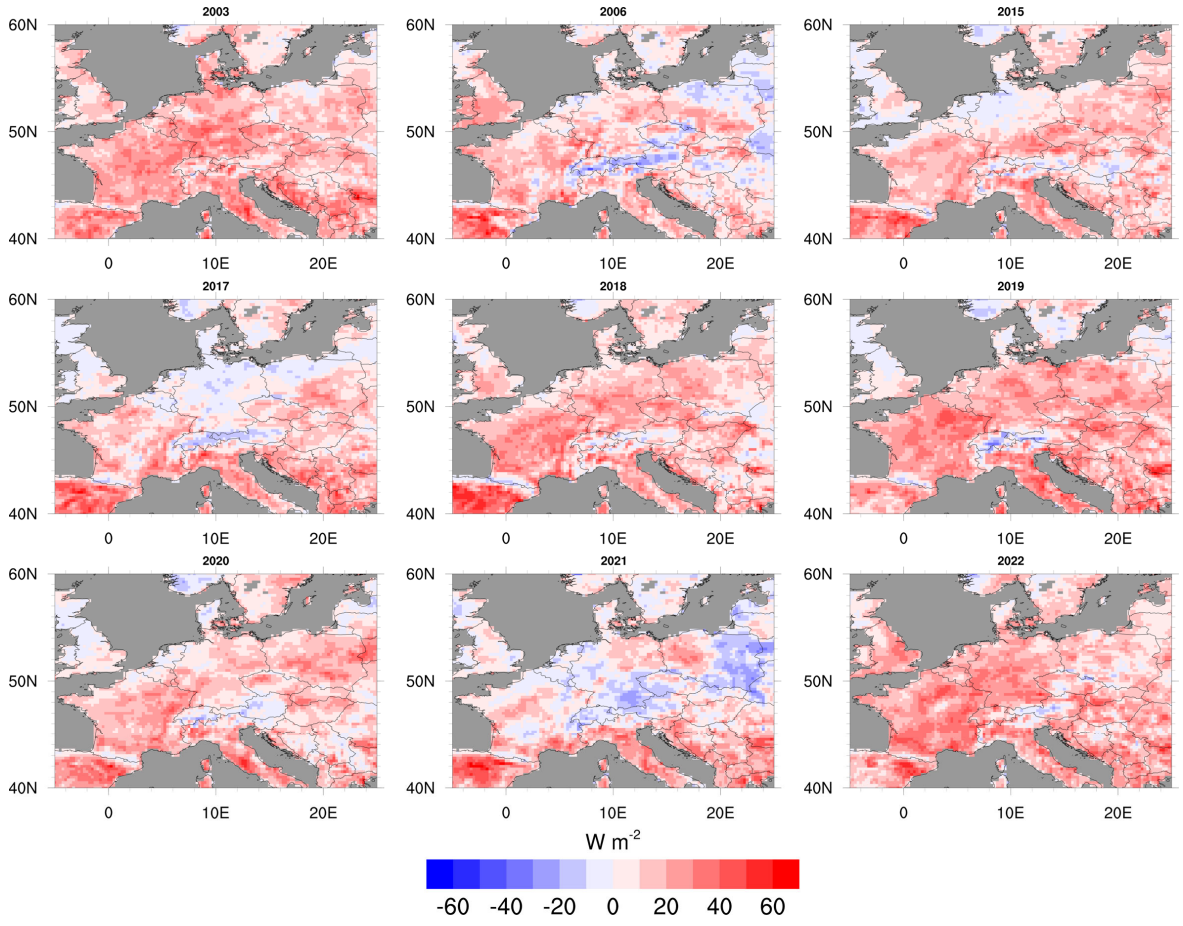

Figure 6. ERA5 based Terrestrial coupling indices (TCI) between root zone soil moisture η and surface latent heat flux (LH) for the selected summer seasons presented in Fig. 1.

4.2 Correlation between LH and SH

During the most hot and dry summers 2003, 2018, 2019 and 2022, the correlation LH-SH (Fig. 7) became negative over Germany, France, and Benelux. which is related to the anomalously warm and dry conditions during these seasons in connection with a soil moisture deficit. This deficit limits LH (Fig. 7) while SH is further increased. During the other years, the correlation largely resembles the TCI pattern (Fig. 6). The pattern for the 2021 is similar as during the cold and wet seasons 1997 and 2002 (Fig. S7) where enough soil moisture is available for evapotranspiration.

The correlation over the Iberian Peninsula is mostly negative which could be related to very low absolute evapotranspiration (Seneviratne et al., 2006).

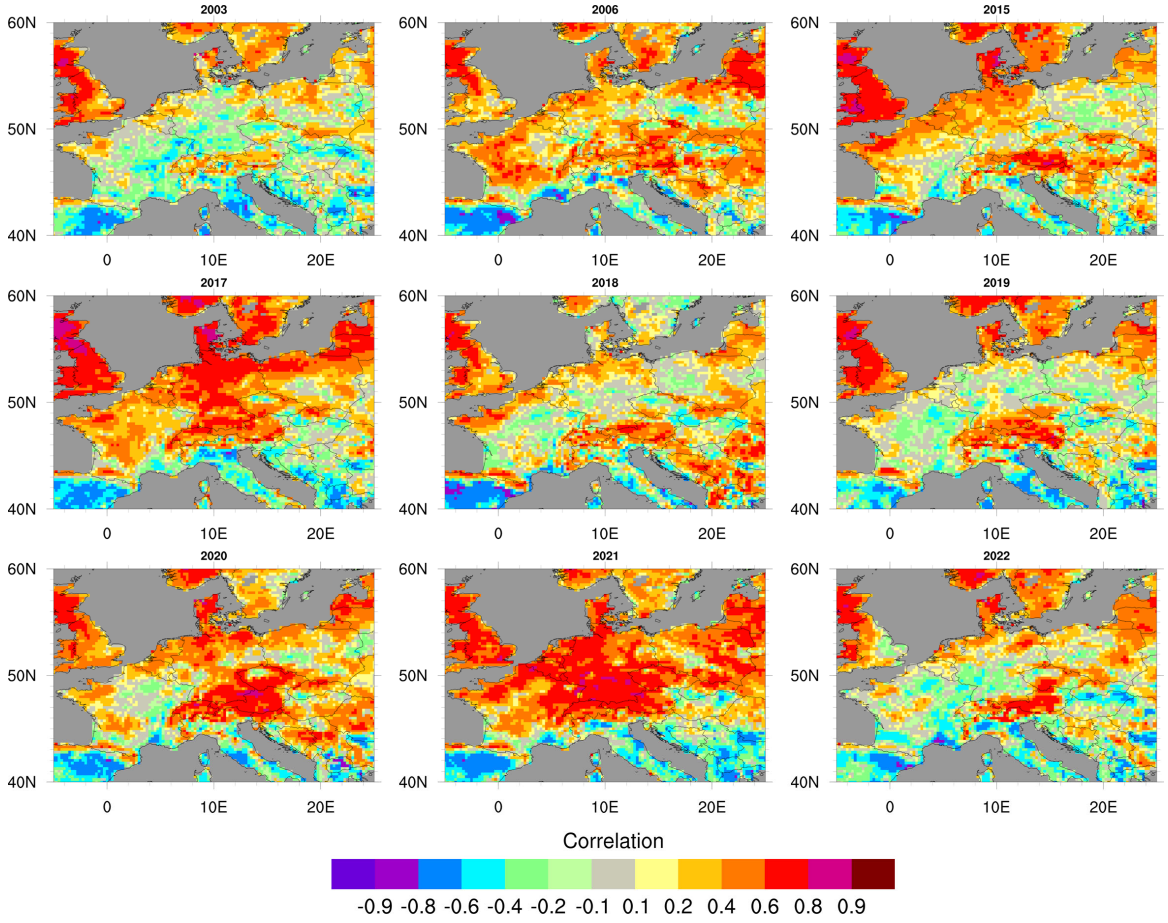

Figure 7. Pearson correlation coefficient between SH and LH for the selected summer seasons presented in Fig. 1. Dark grey areas denote water grid cells.

4.3 Atmospheric Coupling strength and LCL deficit

This section presents two ACIs of the different summer seasons 1991-2022. ACIs are computed 1) between LH and convective available potential energy (CAPE), and 2) between LH and height of the lifted condensation level (HLCL).

CAPE depends on the atmospheric humidity which is, among others, related to LH while LH is related to the atmospheric temperature, humidity, soil moisture and LAI. Thus, an increase in LH leads to an increase of CAPE which indicates the potential for convective developments and thus precipitation.

Positive ACI values denote a dependence of the diurnal evolution of CAPE on the LH evolution while negative values show that CAPE is independent of the LH evolution but dependent on the atmospheric stratification. The lifted condensation level is the level above which saturation occurs and it sinks with increasing atmospheric humidity. Hence, negative ACI values denote a physical relationship between LH and HLCL, whereas a positive index signifies no coupling.

To complement the analysis, the LCL deficit is shown in addition. The LCL deficit can be seen as a proxy for the evolution of the convective atmosphere as a positive LCL deficit inhibits convection developments (Santanello et al., 2009).

Figure 8 shows the ACI between LH and CAPE using daytime data between 06 UTC and 18 UTC.

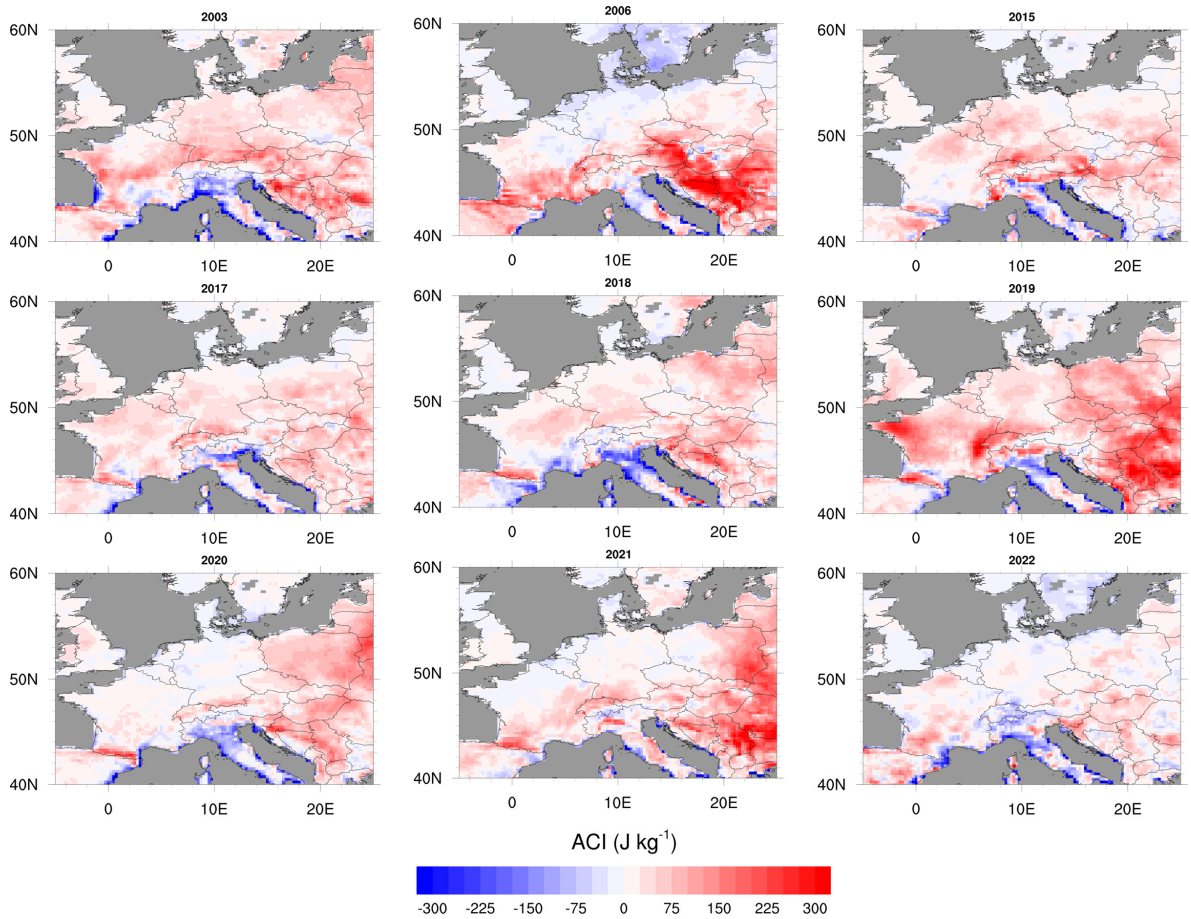

Figure 8. ERA5 based ACI between LH and CAPE. Grey areas denote water grid points.

A common feature is the negative ACI along the coast of the Mediterranean. As the sea surface temperatures in this region can reach up to 26°C (García-Monteiro et al., 2022), this leads to high evaporation over the sea and thus high precipitable water values. Together with a temperature gradient of up to 30 K or more in the Mediterranean between 850 hPa and 500 hPa (not shown), this leads to stronger atmospheric instability and thus reduced coupling to LH.

Coupling hot spots are observed over East and Southeast Europe with ACI values of more than 250 J kg^{-1} occurring in connection with neutral or positive soil moisture anomalies in 2006, 2019, 2020, and 2021 (Fig. 8) which is connected to higher values of LH over these regions due to neutral or positive root zone soil moisture anomalies (Fig. 5). These coupling hot spots were also observed in a climate sensitivity study of Jach et al. (2022) who added climate change signals of temperature and moisture to a RCM simulation. Over Germany and France, mostly only

weak coupling is seen with stronger signals during e2003 and 2019. In case evapotranspiration is not limited by soil moisture, the incoming radiation is allowing for potential evapotranspiration and surface latent and sensible heat fluxes are partitioned accordingly. In case evapotranspiration is not limited by incoming radiation but by available soil moisture evapotranspiration is below the potential rate leading to higher Bowen ratios. The increasing Bowen ratio leads to an increase in temperature. This enhances evapotranspiration and therefore a gradual decrease in soil moisture towards wilting point. According to Benson and Dirmeyer (2021) this ultimately leads to the situation that latent heat fluxes almost vanish and the incoming radiation mainly transforms into sensible heat which can exacerbate heatwaves and droughts.

The LCL deficit (Fig. 9) is usually positive over South Europe leading to a strong inhibition of the formation of clouds and precipitation. Over Central Europe the LCL deficit is comparatively small with values of up to 300 m, unlike the years 2003and 2022 which show strong positive values. These are the summers with a pronounced negative soil moisture anomaly and a strong positive temperature anomaly of more than 3°C (Fig. 2). Hence, HLCL is higher than the planetary boundary layer height potentially leading to clear sky conditions and thus inhibiting convection (Santanello et al., 2011). As the TCI is mostly positive over these regions during these summers, while the ACI is neutral to slightly positive, this indicates that soil moisture variation impacts LH variations but with weak feedback to the atmosphere as indicated by the TLCI (Dirmeyer et al., 2014 , Fig. S3).

The LCL deficit over the British Isles and South Scandinavia, stays negative throughout all summer seasons. As at the same time the ACI between LH and CAPE shows also only small values, this suggests that the British Isles and South Scandinavia are more frequently impacted by large scale synoptic systems with a more stable atmosphere rather than localized precipitation events (Jach et al., 2020) .

To complement our analysis, Fig. 10 shows the ACI between LH and HLCL. Over Germany, France, and Benelux, the ACI shows low or negative values during the extreme warm and dry years 2003, 2018, and 2022.

This indicates that the very dry soil during these summers (Fig. 5) caused the low LH which in turn initiated a considerable increase of the HLCL (Fig. S4). At the same time, the high SH (not shown) leads to an increase of the PBL height and thus a higher LCL deficit as shown in Fig. 9. In 2006, 2015, and 2017 the ACI is positive over large parts of Central Europe indicating that LH variations drive the development of HLCL, During summer 2021, which showed record high temperatures over Europe, Central Europe shows a positive soil moisture anomaly (Fig. 5) connected to weak or negative coupling between η and LH (Fig. 6). This means that LH shows little variations and thus lowering HLCL (Wei et al., 2021) which is also reflected in a neutral LCL deficit Fig. 9).

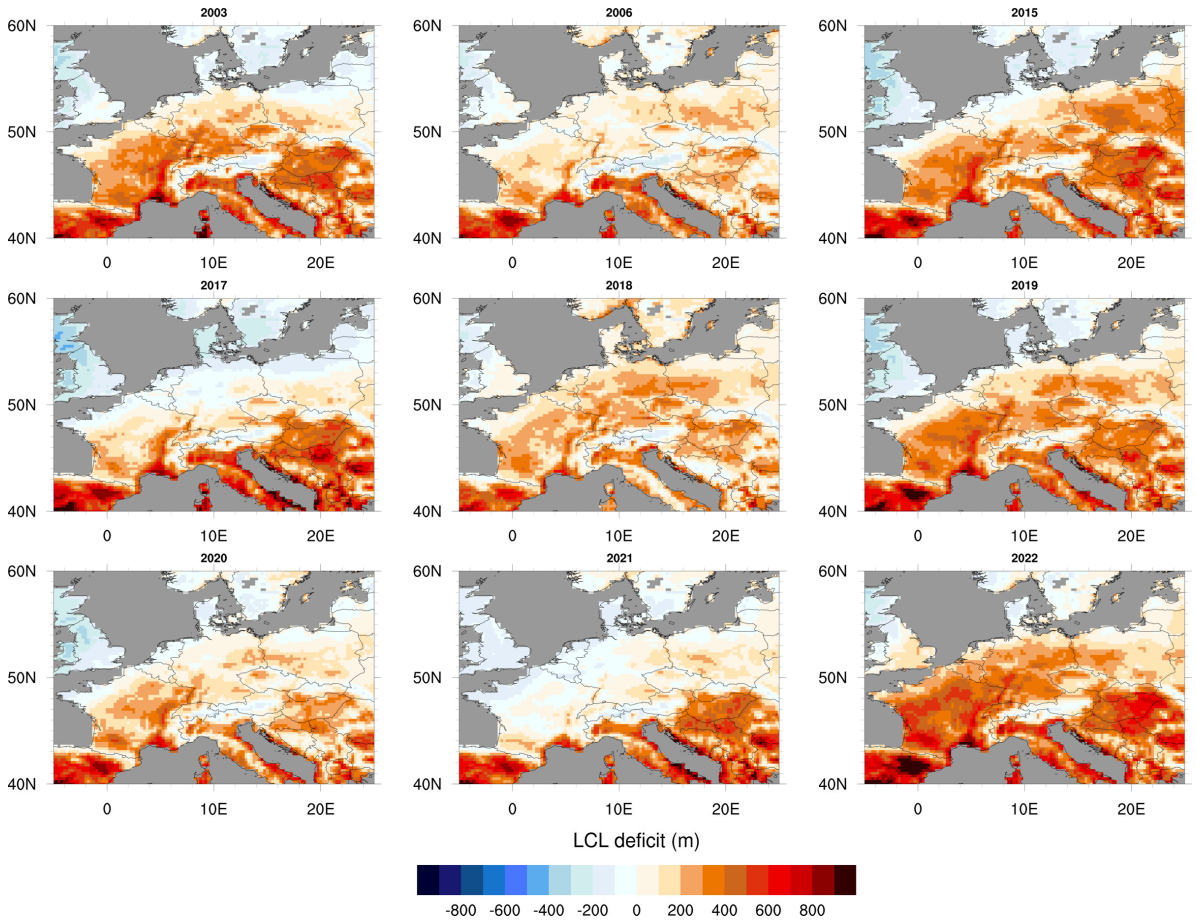

Figure 9. Mean ERA5 LCL deficit. Orange and reddish colors denote less favorable conditions for convection.

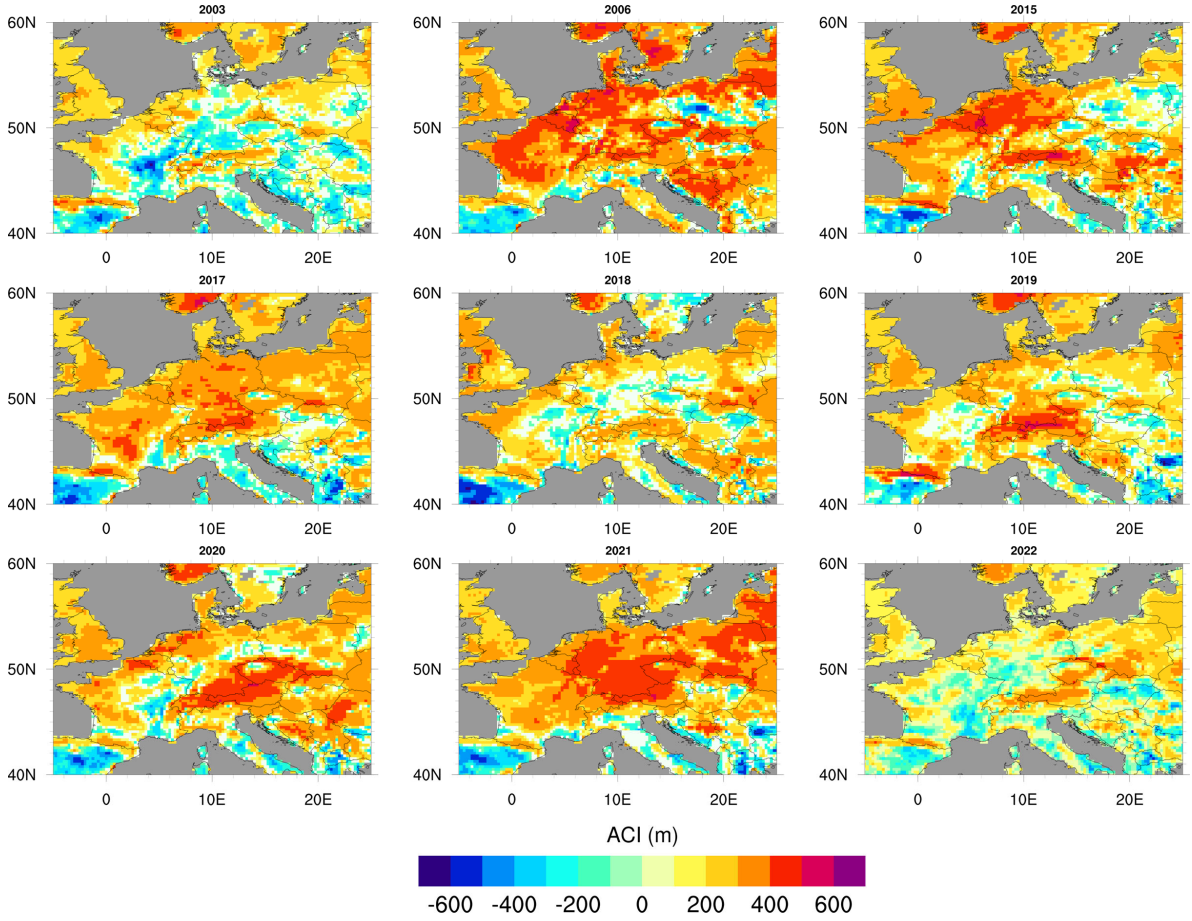

Figure 10. ACI LH-HLCL for the selected summer seasons.

5 Discussion

During the warm summer seasons shown in this study, the TCI η-LH shows a strong coupling throughout major parts of Europe (Fig. 6) indicating that variations of η drive LH which was also observed in a study of Warrach-Sagi et al. (2022). A common feature of all evaluated summer seasons is the anticorrelation of LH and SH south of 44 °N (Fig. 7). These regions are usually water-limited thus leading to limited evapotranspiration further reducing LH. As enough incoming energy is present, this further enhances SH and thus could further intensify drought periods in these regions.

Together with the positive TCI this points to a strong limitation of evapotranspiration by insufficient root zone soil moisture resulting in low LAI which is usually the case in South Europe (see Fig. S5c,d). At the same time, the correlation between SH and LH is shows a heterogenous pattern. The correlation between SH and LH is mainly positive over the British Isles, pointing s towards that evapotranspiration is limited by the incoming energy (Knist et al., 2017) which is also the case over France, Benelux, and Germany for summer 2021. .

2018 started with an already warmer than average and slightly drier spring season over Germany (Xoplaki et al., 2023) leading to a severe drought due to a strong soil moisture depletion (Rousi et al., 2023) resulting in an exceptionally low LAI (Fig. S5c). Dirmeyer et al. (2021) found that when the volumetric soil moisture content falls below a critical value, surface heating becomes extremely more sensitive to further surface drying amplifying the intensity of heatwaves. A strong SW-NE temperature anomaly gradient associated with a strong positive 500

hPa geopotential anomaly north of 55°N was evident in 2021. A major event during this summer was the flood event mid of July 2021 which affected larger areas of West and Central Europe and lead to extreme precipitation of more than 150 mm d^{-1} (Ludwig et al., 2023; Mohr et al., 2023). This heavy precipitation event, which was also captured by ERA5 (Fig. 4), was caused by a slow moving small-scale low-pressure system and led to longer lasting positive soil moisture anomaly. The anomaly is directly reflected in low TCI values and a strong correlation between LH and SH as enough surface moisture was available for evaporation.

The ACI LH-CAPE shows coupling hot-spots over Southeast and East Europe as well as over the Baltic states which were also observed in the study of Jach et al. (2022) who applied a climate temperature change signal to an existing 30 year simulation and evaluated the CTP-HI_{low} feedback metric (Findell and Eltahir, 2003b, 2003a). In contrast to the cold and wet years 1997 and 2002 (Figs. S6, S7), the LCL deficit (not shown) is mostly positive over Central and South Europe which is associated with a negative precipitation anomaly over the respective areas. On the other hand, the negative LCL deficit over the British Isles is directly connected with a positive precipitation anomaly (especially 2019 and 2020) indicating that LA feedback processes were driven by low pressure systems.

Currently, ERA5 applies a static LAI climatology (Fig. S5b) which was derived from the period 2000-2008 (Boussetta et al., 2013; ECMWF, 2016). However, under a changing climate the interannual variability of LAI is increasing as observed by satellites in the Copernicus Global Land Service (CGLS) project (Fuster et al., 2020) (Fig. S5c,d). Data such as these could help to further improve, e.g., the simulated evapotranspiration.

A study of Denissen et al. (2020) found that LSMs tend to overestimate the critical soil moisture and thus evaporation becomes soil moisture limited too early. A recent study of Warrach-Sagi et al. (2022) using the LSM NOAH-MP (Niu et al., 2011) showed that, even on a convection permitting (CP) horizontal resolution, LA feedback strength tends to be underestimated when using a LAI climatology in numerical weather prediction (NWP) models as compared to including the dynamic vegetation model GECROS (Yin and van Laar, 2005). This is in contrast to the results of Denissen et al. (2020) indicating the need for further enhancements of the applied LSMs (Hersbach and Bell, 2022; He et al., 2023).

Martens et al. (2020) evaluated surface latent heat fluxes from ERA5 against FLUXNET stations (Pastorello et al., 2020) for the period 1991-2014. Their analysis revealed that ERA5 surface fluxes perform well in moderate temperature climate which is the case over Europe. ERA5 soil moisture over Europe shows a reasonable correlation of up to 0.7 over Europe (Muñoz-Sabater et al., 2021) while LH in ERA5 tend to be overestimated on average by about 9 W m^{-2} when compared to all stations. This could be related to an overestimation of wet days in combination with underestimated sub-daily precipitation rates (Beck et al., 2019). The tendency to overestimate precipitation resulting in higher LH estimates could lead to an increased atmospheric instability and thus affecting the TCI, ACI and the LCL deficit.

6 Summary

This paper describes the variability of the LA coupling strength of the warm summer seasons 1991-2022 which became the dominant situation over Europe since 2010. The summer seasons were selected according to 2-m temperature anomalies based on ERA5 (Hersbach et al., 2020) with respect to 1991-2020 (WMO, 2017). To further support our analysis, anomalies of the 500 hPa geopotential, volumetric root zone soil moisture, and precipitation anomalies, derived from ERA5, were considered. In addition, we also used the E-OBS precipitation data set (Cornes et al., 2018) for the interpretation of our results.

The analysis of the LA coupling strength was performed by means of different indices (Dirmeyer, 2011; Santanello et al., 2018) and by applying the coupling metrics framework provided by Tawfik (2015). All indices were calculated from ERA5 data using daytime values between 06 UTC and 18 UTC for each day (Yin et al., 2023).

According to Rousi et al. (2022) the frequency of the occurrence of heat waves has been accelerating over Europe in the last 30-40 years where the large-scale circulation pattern often features mid- and upper troposphere blocking situations leading to a split of the jet stream towards the Arctic and the Mediterranean. As the jet stream is an important feature for the European weather, it can also alter the near surface flow conditions in West and Central Europe (Laurila et al., 2021) while in other regions like the Mediterranean and East Europe, soil moisture preconditioning is more important as the impact of the jet stream becomes weaker (Prodhomme et al., 2022).

Our results revealed that warm and dry summers are characterized by positive geopotential anomalies throughout Europe (Kueh and Lin, 2020; Rousi et al., 2023) while the two warm and wet summers exhibit a negative geopotential anomaly over Central Europe (not shown). Strong geopotential anomalies are linked to considerable positive 2-m temperature anomalies and the warm and dry summer seasons are usually characterized by a strong dry soil moisture anomaly.

Our results show that the interannual temperature and soil moisture variability during the different summers considerably drive the interannual variability in LA coupling over Central Europe. Hot and dry conditions shift the terrestrial coupling to the moisture-limited regime, push the sensitivity of the HLCL on low LH, and through this switch gears to strongly positive LCL deficits which decreases the likelihood for locally triggered deep convection in this region. The increasing frequency of warm and dry years toward the second half of the study period hints toward a trend of extended periods of moisture-limitations for evapotranspiration. By applying the offline mesoscale hydrology model (mHM, Samaniego et al., 2010), Markonis et al. (2021) found a considerable increase in the number of drought events over Central Europe since 2010 which they relate to increasing temperature, lack of rainfall resulting in a soil moisture depletion due to excessive evapotranspiration during spring. This suggests a growing influence of soil moisture variability on the meteorological conditions which was not as pronounced in the first half of the period 1991-2020 experiencing cooler and moister conditions.

From our study we conclude that applying reanalysis data for the derivation of the feedback metrics could be used as a reference for further analyses and evaluation of climate simulations. However, this requires high-frequency model output from (high-resolution) climate models (Findell et al., 2024) which is still a challenging task.

Though it requires more research to deepen the understanding of how different surface wind patterns, horizontal moisture transport (Findell et al., 2024), the location of the center of a high- or low-pressure system influence the coupling or how dynamic vegetation-climate feedback do (Nogueira et al., 2021; Warrach-Sagi et al., 2022), we consider this work a valuable contribution to further understanding land surface influences on extreme events over Central Europe.

Acknowledgements

This work was funded by the German Ministry of Education and Research (BMBF) project ClimXtreme (subproject LAFEP, grant number 01LP1902D). Copernicus Climate Change Service (2018) data was downloaded from the Copernicus Climate Change Service (C3S) Climate Data Store https://cds.climate.copernicus.eu/cdsapp#!/dataset/reanalysis-era5-single-levels?tab=overview. The results

contain modified Copernicus Climate Change Service information 2020. Neither the European Commission nor ECMWF is responsible for any use that may be made of the Copernicus information or data it contains.

Code availability

The code used in this study to calculate the coupling indices is obtained from https://github.com/abtawfik/coupling-metrics. The NCL software package can be downloaded from https://www.ncl.ucar.edu/current_release.shtml.

Data availability

E-OBS data were downloaded from https://surfobs.climate.copernicus.eu/dataaccess/access_E-OBS.php and the ERA5 data are available at https://cds.climate.copernicus.eu/cdsapp#!/dataset/reanalysis-era5-single-levels?tab=overview.

Author contributions

TS, LJ, VW, and KWS conceived the idea for the LA feedback study presented here. TS processed the data and graphics and performed the analyses together with LJ and KWS. The paper was written by TS with support of all coauthors.

Competing interests

The authors declare that they have no competing interests.

References

Albergel, C., Rosnay, P. de, Balsamo, G., Isaksen, L., and Muñoz-Sabater, J.: Soil Moisture Analyses at ECMWF: Evaluation Using Global Ground-Based In Situ Observations, Journal of Hydrometeorology, 13, 1442–1460, https://doi.org/10.1175/JHM-D-11-0107.1, 2012.

Balsamo, G., Beljaars, A., Scipal, K., Viterbo, P., van den Hurk, B., Hirschi, M., and Betts, A. K.: A Revised Hydrology for the ECMWF Model: Verification from Field Site to Terrestrial Water Storage and Impact in the Integrated Forecast System, Journal of Hydrometeorology, 10, 623–643, https://doi.org/10.1175/2008JHM1068.1, 2009.

Beck, H. E., Wood, E. F., Pan, M., Fisher, C. K., Miralles, D. G., van Dijk, A. I. J. M., McVicar, T. R., and Adler, R. F.: MSWEP V2 Global 3-Hourly 0.1° Precipitation: Methodology and Quantitative Assessment, Bulletin of the American Meteorological Society, 100, 473–500, https://doi.org/10.1175/BAMS-D-17-0138.1, 2019.

Becker, F. N., Fink, A. H., Bissolli, P., and Pinto, J. G.: Towards a more comprehensive assessment of the intensity of historical European heat waves (1979–2019), Atmospheric Science Letters, 23, https://doi.org/10.1002/ASL.1120, 2022.

Benson, D. O. and Dirmeyer, P. A.: Characterizing the Relationship between Temperature and Soil Moisture Extremes and Their Role in the Exacerbation of Heat Waves over the Contiguous United States, Journal of Climate, 34, 2175–2187, https://doi.org/10.1175/JCLI-D-20-0440.1, 2021.

Boeing, F., Rakovec, O., Kumar, R., Samaniego, L., Schrön, M., Hildebrandt, A., Rebmann, C., Thober, S., Müller, S., Zacharias, S., Bogena, H., Schneider, K., Kiese, R., Attinger, S., and Marx, A.: High-resolution drought simulations and comparison to soil moisture observations in Germany, Hydrol. Earth Syst. Sci., 26, 5137–5161, https://doi.org/10.5194/hess-26-5137-2022, 2022.

Bollmeyer, C., Keller, J. D., Ohlwein, C., Wahl, S., Crewell, S., Friederichs, P., Hense, A., Keune, J., Kneifel, S., Pscheidt, I., Redl, S., and Steinke, S.: Towards a high-resolution regional reanalysis for the European CORDEX domain, Q.J.R. Meteorol. Soc., 141, 1–15, https://doi.org/10.1002/qj.2486, 2015.

Bolton, D.: The Computation of Equivalent Potential Temperature, Mon. Wea. Rev., 108, 1046–1053, https://doi.org/10.1175/1520-0493(1980)108<1046:TCOEPT>2.0.CO;2, 1980.

Boussetta, S., Balsamo, G., Beljaars, A., Kral, T., and Jarlan, L.: Impact of a satellite-derived leaf area index monthly climatology in a global numerical weather prediction model, International Journal of Remote Sensing, 34, 3520–3542, https://doi.org/10.1080/01431161.2012.716543, 2013.

Brown, D., Brownrigg, R., Haley, M., and Huang, W.: NCAR Command Language (NCL), UCAR/NCAR - Computational and Information Systems Laboratory (CISL), 2012.

C3S: European State of the Climate 2022, Summary, Copernicus Climate Change Service, https://doi.org/10.24381/gvaf-h066, last access: 18 July 2023, 2023.

C3S: European State of the Climate 2021 summary, Copernicus Climate Change Service, https://doi.org/10.21957/9d7g-hn83, last access: 15 February 2024, 2022.

C3S: European State of the Climate 2018, Copernicus Climate Change Service, https://climate.copernicus.eu/ESOTC/2018, last access: 15 February 2024, 2018.

Copernicus Climate Change Service: ERA5 hourly data on single levels from 1959 to present, 2018.

Cornes, R. C., van der Schrier, G., van den Besselaar, E. J. M., and Jones, P. D.: An Ensemble Version of the E-OBS Temperature and Precipitation Data Sets, J. Geophys. Res. Atmos., 123, 9391–9409, https://doi.org/10.1029/2017JD028200, available at: https://agupubs.onlinelibrary.wiley.com/doi/full/10.1029/2017JD028200, 2018.

Dee, D. P., Uppala, S. M., Simmons, A. J., Berrisford, P., Poli, P., Kobayashi, S., Andrae, U., Balmaseda, M. A., Balsamo, G., Bauer, P., Bechtold, P., Beljaars, A. C. M., van de Berg, L., Bidlot, J., Bormann, N., Delsol, C., Dragani, R., Fuentes, M., Geer, A. J., Haimberger, L., Healy, S. B., Hersbach, H., Hólm, E. V., Isaksen, L., Kållberg, P., Köhler, M., Matricardi, M., McNally, A. P., Monge-Sanz, B. M., Morcrette, J.-J., Park, B.-K., Peubey, C., Rosnay, P. de, Tavolato, C., Thépaut, J.-N., and Vitart, F.: The ERA-Interim reanalysis: configuration and performance of the data assimilation system, Q.J.R. Meteorol. Soc., 137, 553–597, https://doi.org/10.1002/qj.828, 2011.

Denissen, J. M. C., Teuling, A. J., Pitman, A. J., Koirala, S., Migliavacca, M., Li, W., Reichstein, M., Winkler, A. J., Zhan, C., and Orth, R.: Widespread shift from ecosystem energy to water limitation with climate change, Nat. Clim. Chang., 12, 677–684, https://doi.org/10.1038/s41558-022-01403-8, 2022.

Denissen, J. M., Teuling, A. J., Reichstein, M., and Orth, R.: Critical Soil Moisture Derived From Satellite Observations Over Europe, Journal of Geophysical Research: Atmospheres, 125, https://doi.org/10.1029/2019JD031672, 2020.

Di Capua, G., Sparrow, S., Kornhuber, K., Rousi, E., Osprey, S., Wallom, D., van den Hurk, B., and Coumou, D.: Drivers behind the summer 2010 wave train leading to Russian heatwave and Pakistan flooding, npj Clim Atmos Sci, 4, https://doi.org/10.1038/s41612-021-00211-9, 2021.

Dirmeyer, P. A.: The terrestrial segment of soil moisture-climate coupling, Geophys. Res. Lett., 38, n/a-n/a, https://doi.org/10.1029/2011GL048268, 2011.

Dirmeyer, P. A., Balsamo, G., Blyth, E. M., Morrison, R., and Cooper, H. M.: Land-Atmosphere Interactions Exacerbated the Drought and Heatwave Over Northern Europe During Summer 2018, AGU Advances, 2, https://doi.org/10.1029/2020AV000283, 2021.

Dirmeyer, P. A., Wang, Z., Mbuh, M. J., and Norton, H. E.: Intensified land surface control on boundary layer growth in a changing climate, Geophys. Res. Lett., 41, 1290–1294, https://doi.org/10.1002/2013GL058826, 2014.

Duan, S. Q., Findell, K. L., and Wright, J. S.: Three Regimes of Temperature Distribution Change Over Dry Land, Moist Land, and Oceanic Surfaces, Geophys. Res. Lett., 47, https://doi.org/10.1029/2020GL090997, 2020.

ECMWF: IFS Documentation CY41R2 - Part IV: Physical Processes, 2016.

Findell, K. L. and Eltahir, E. A. B.: Atmospheric Controls on Soil Moisture–Boundary Layer Interactions. Part I: Framework Development, Journal of Hydrometeorology, 4, 552–569, https://doi.org/10.1175/1525-7541(2003)004%3C0552:ACOSML%3E2.0.CO;2, 2003a.

Findell, K. L. and Eltahir, E. A. B.: Atmospheric Controls on Soil Moisture–Boundary Layer Interactions. Part II: Feedbacks within the Continental United States, Journal of Hydrometeorology, 4, 570–583, https://doi.org/10.1175/1525-7541(2003)004%3C0570:ACOSML%3E2.0.CO;2, 2003b.

Findell, K. L., Yin, Z., Seo, E., Dirmeyer, P. A., Arnold, N. P., Chaney, N., Fowler, M. D., Huang, M., Lawrence, D. M., Ma, P.-L., and Santanello Jr., J. A.: Accurate assessment of land–atmosphere coupling in climate models requires high-frequency data output, Geosci. Model Dev., 17, 1869–1883, https://doi.org/10.5194/gmd-17-1869-2024, 2024.

Findell, K. L., Gentine, P., Lintner, B. R., and Guillod, B. P.: Data Length Requirements for Observational Estimates of Land–Atmosphere Coupling Strength, Journal of Hydrometeorology, 16, 1615–1635, https://doi.org/10.1175/JHM-D-14-0131.1, 2015.

Fuster, B., Sánchez-Zapero, J., Camacho, F., García-Santos, V., Verger, A., Lacaze, R., Weiss, M., Baret, F., and Smets, B.: Quality Assessment of PROBA-V LAI, fAPAR and fCOVER Collection 300 m Products of Copernicus Global Land Service, Remote Sensing, 12, 1017, https://doi.org/10.3390/rs12061017, 2020.

García-Herrera, R., Díaz, J., Trigo, R. M., Luterbacher, J., and Fischer, E. M.: A Review of the European Summer Heat Wave of 2003, Critical Reviews in Environmental Science and Technology, 40, 267–306, https://doi.org/10.1080/10643380802238137, 2010.

García-Monteiro, S., Sobrino, J. A., Julien, Y., Sòria, G., and Skokovic, D.: Surface Temperature trends in the Mediterranean Sea from MODIS data during years 2003–2019, Regional Studies in Marine Science, 49, 102086, https://doi.org/10.1016/j.rsma.2021.102086, 2022.

Georgakakos, K. P. and Bras, R. L.: A hydrologically useful station precipitation model: 1. Formulation, Water Resour. Res., 20, 1585–1596, https://doi.org/10.1029/WR020i011p01585, 1984.

Guo, Z. and Dirmeyer, P. A.: Interannual Variability of Land–Atmosphere Coupling Strength, Journal of Hydrometeorology, 14, 1636–1646, https://doi.org/10.1175/JHM-D-12-0171.1, 2013.

Guo, Z., Dirmeyer, P. A., Koster, R. D., Sud, Y. C., Bonan, G., Oleson, K. W., Chan, E., Verseghy, D., Cox, P., Gordon, C. T., McGregor, J. L., Kanae, S., Kowalczyk, E., Lawrence, D., Liu, P., Mocko, D., Lu, C.-H., Mitchell, K., Malyshev, S., McAvaney, B., Oki, T., Yamada, T., Pitman, A., Taylor, C. M., Vasic, R., and

Xue, Y.: GLACE: The Global Land–Atmosphere Coupling Experiment. Part II: Analysis, Journal of Hydrometeorology, 7, 611–625, https://doi.org/10.1175/JHM511.1, 2006.

Hauser, M., Orth, R., and Seneviratne, S. I.: Role of soil moisture versus recent climate change for the 2010 heat wave in western Russia, Geophys. Res. Lett., 43, 2819–2826, https://doi.org/10.1002/2016GL068036, 2016.

He, C., Valayamkunnath, P., Barlage, M., Chen, F., Gochis, D., Cabell, R., Schneider, T., Rasmussen, R., Niu, G.-Y., Yang, Z.-L., Niyogi, D., and Ek, M.: Modernizing the open-source community Noah-MP land surface model (version 5.0) with enhanced modularity, interoperability, and applicability, 2023.

Hersbach, H. and Bell, B.: Characteristics of ERA5 and innovations for ERA6, 5th C3S General Assembly, https://climate.copernicus.eu/sites/default/files/2022-09/S3_Hans_Hersbach_v1.pdf, last access: 4 July 2023, 2022.

Hersbach, H., Bell, B., Berrisford, P., Hirahara, S., Horányi, A., Muñoz-Sabater, J., Nicolas, J., Peubey, C., Radu, R., Schepers, D., Simmons, A., Soci, C., Abdalla, S., Abellan, X., Balsamo, G., Bechtold, P., Biavati, G., Bidlot, J., Bonavita, M., Chiara, G., Dahlgren, P., Dee, D., Diamantakis, M., Dragani, R., Flemming, J., Forbes, R., Fuentes, M., Geer, A., Haimberger, L., Healy, S., Hogan, R. J., Hólm, E., Janisková, M., Keeley, S., Laloyaux, P., Lopez, P., Lupu, C., Radnoti, G., Rosnay, P., Rozum, I., Vamborg, F., Villaume, S., and Thépaut, J.-N.: The ERA5 global reanalysis, Q.J.R. Meteorol. Soc., 146, 1999–2049, https://doi.org/10.1002/qj.3803, 2020.

Huebener, H., Hoffmann, P., Keuler, K., Pfeifer, S., Ramthun, H., Spekat, A., Steger, C., and Warrach-Sagi, K.: Deriving user-informed climate information from climate model ensemble results, Adv. Sci. Res., 14, 261–269, https://doi.org/10.5194/asr-14-261-2017, 2017.

Jach, L., Schwitalla, T., Branch, O., Warrach-Sagi, K., and Wulfmeyer, V.: Sensitivity of land–atmosphere coupling strength to changing atmospheric temperature and moisture over Europe, Earth Syst. Dynam., 13, 109–132, https://doi.org/10.5194/esd-13-109-2022, 2022.

Jach, L., Warrach-Sagi, K., Ingwersen, J., Kaas, E., and Wulfmeyer, V.: Land Cover Impacts on Land-Atmosphere Coupling Strength in Climate Simulations With WRF Over Europe, Journal of Geophysical Research: Atmospheres, 125, https://doi.org/10.1029/2019JD031989, 2020.

Knist, S., Goergen, K., Buonomo, E., Christensen, O. B., Colette, A., Cardoso, R. M., Fealy, R., Fernández, J., García-Díez, M., Jacob, D., Kartsios, S., Katragkou, E., Keuler, K., Mayer, S., van Meijgaard, E., Nikulin, G., Soares, P. M. M., Sobolowski, S., Szepszo, G., Teichmann, C., Vautard, R., Warrach-Sagi, K., Wulfmeyer, V., and Simmer, C.: Land-atmosphere coupling in EURO-CORDEX evaluation experiments, J. Geophys. Res. Atmos., 122, 79–103, https://doi.org/10.1002/2016JD025476, 2017.

Kornhuber, K., Petoukhov, V., Petri, S., Rahmstorf, S., and Coumou, D.: Evidence for wave resonance as a key mechanism for generating high-amplitude quasi-stationary waves in boreal summer, Clim Dyn, 49, 1961–1979, https://doi.org/10.1007/s00382-016-3399-6, 2017.

Koster, R. D., Dirmeyer, P. A., Guo, Z., Bonan, G., Chan, E., Cox, P., Gordon, C. T., Kanae, S., Kowalczyk, E., Lawrence, D., Liu, P., Lu, C.-H., Malyshev, S., McAvaney, B., Mitchell, K., Mocko, D., Oki, T., Oleson, K., Pitman, A., Sud, Y. C., Taylor, C. M., Verseghy, D., Vasic, R., Xue, Y., and Yamada, T.: Regions of strong coupling between soil moisture and precipitation, Science (New York, N.Y.), 305, 1138–1140, https://doi.org/10.1126/science.1100217, 2004.

Kueh, M.-T. and Lin, C.-Y.: The 2018 summer heatwaves over northwestern Europe and its extended-range prediction, Scientific reports, 10, 19283, https://doi.org/10.1038/s41598-020-76181-4, 2020.

Laurila, T. K., Sinclair, V. A., and Gregow, H.: Climatology, variability, and trends in near-surface wind speeds over the North Atlantic and Europe during 1979–2018 based on ERA5, Int J Climatol, 41, 2253–2278, https://doi.org/10.1002/joc.6957, 2021.

Lavers, D. A., Simmons, A., Vamborg, F., and Rodwell, M. J.: An evaluation of ERA5 precipitation for climate monitoring, Q.J.R. Meteorol. Soc., 148, 3152–3165, https://doi.org/10.1002/qj.4351, 2022.

Leutwyler, D., Imamovic, A., and Schär, C.: The Continental-Scale Soil-Moisture Precipitation Feedback in Europe with Parameterized and Explicit Convection, Journal of Climate, 1–56, https://doi.org/10.1175/JCLI-D-20-0415.1, 2021.

Lhotka, O. and Kyselý, J.: The 2021 European Heat Wave in the Context of Past Major Heat Waves, Earth and Space Science, 9, https://doi.org/10.1029/2022EA002567, 2022.

Lo, M.-H., Wu, W.-Y., Tang, L. I., Ryu, D., Rashid, M., and Wu, R.-J.: Temporal Changes in Land Surface Coupling Strength: An Example in a Semi-Arid Region of Australia, Journal of Climate, 34, 1503–1513, https://doi.org/10.1175/JCLI-D-20-0250.1, 2021.

Ludwig, P., Ehmele, F., Franca, M. J., Mohr, S., Caldas-Alvarez, A., Daniell, J. E., Ehret, U., Feldmann, H., Hundhausen, M., Knippertz, P., Küpfer, K., Kunz, M., Mühr, B., Pinto, J. G., Quinting, J., Schäfer, A. M., Seidel, F., and Wisotzky, C.: A multi-disciplinary analysis of the exceptional flood event of July 2021 in central Europe – Part 2: Historical context and relation to climate change, Nat. Hazards Earth Syst. Sci., 23, 1287–1311, https://doi.org/10.5194/nhess-23-1287-2023, 2023.

Markonis, Y., Kumar, R., Hanel, M., Rakovec, O., Máca, P., and AghaKouchak, A.: The rise of compound warm-season droughts in Europe, Science Advances, 7, https://doi.org/10.1126/sciadv.abb9668, 2021.

Martens, B., Schumacher, D. L., Wouters, H., Muñoz-Sabater, J., Verhoest, N. E. C., and Miralles, D. G.: Evaluating the land-surface energy partitioning in ERA5, Geosci. Model Dev., 13, 4159–4181, https://doi.org/10.5194/gmd-13-4159-2020, 2020.

Miralles, D. G., Gentine, P., Seneviratne, S. I., and Teuling, A. J.: Land-atmospheric feedbacks during droughts and heatwaves: state of the science and current challenges, Annals of the New York Academy of Sciences, 1436, 19–35, https://doi.org/10.1111/nyas.13912, 2019.

Miralles, D. G., Teuling, A. J., van Heerwaarden, C. C., and Vilà-Guerau de Arellano, J.: Mega-heatwave temperatures due to combined soil desiccation and atmospheric heat accumulation, Nat. Geosci., 7, 345–349, https://doi.org/10.1038/ngeo2141, 2014.

Mohr, S., Ehret, U., Kunz, M., Ludwig, P., Caldas-Alvarez, A., Daniell, J. E., Ehmele, F., Feldmann, H., Franca, M. J., Gattke, C., Hundhausen, M., Knippertz, P., Küpfer, K., Mühr, B., Pinto, J. G., Quinting, J., Schäfer, A. M., Scheibel, M., Seidel, F., and Wisotzky, C.: A multi-disciplinary analysis of the exceptional flood event of July 2021 in central Europe – Part 1: Event description and analysis, Nat. Hazards Earth Syst. Sci., 23, 525–551, https://doi.org/10.5194/nhess-23-525-2023, 2023.

Müller, O. V., Vidale, P. L., Vannière, B., Schiemann, R., Senan, R., Haarsma, R. J., and Jungclaus, J. H.: Land–Atmosphere Coupling Sensitivity to GCMs Resolution: A Multimodel Assessment of Local and Remote Processes in the Sahel Hot Spot, Journal of Climate, 34, 967–985, https://doi.org/10.1175/JCLI-D-20-0303.1, 2021.

Muñoz-Sabater, J., Dutra, E., Agustí-Panareda, A., Albergel, C., Arduini, G., Balsamo, G., Boussetta, S., Choulga, M., Harrigan, S., Hersbach, H., Martens, B., Miralles, D. G., Piles, M., Rodríguez-Fernández, N.

J., Zsoter, E., Buontempo, C., and Thépaut, J.-N.: ERA5-Land: a state-of-the-art global reanalysis dataset for land applications, Earth Syst. Sci. Data, 13, 4349–4383, https://doi.org/10.5194/essd-13-4349-2021, 2021.

Niu, G.-Y., Yang, Z.-L., Mitchell, K. E., Chen, F., Ek, M. B., Barlage, M., Kumar, A., Manning, K., Niyogi, D., Rosero, E., Tewari, M., and Xia, Y.: The community Noah land surface model with multiparameterization options (Noah-MP): 1. Model description and evaluation with local-scale measurements, J. Geophys. Res., 116, https://doi.org/10.1029/2010JD015139, 2011.

Nogueira, M., Boussetta, S., Balsamo, G., Albergel, C., Trigo, I. F., Johannsen, F., Miralles, D. G., and Dutra, E.: Upgrading Land-Cover and Vegetation Seasonality in the ECMWF Coupled System: Verification With FLUXNET Sites, METEOSAT Satellite Land Surface Temperatures, and ERA5 Atmospheric Reanalysis, J. Geophys. Res. Atmos., 126, e2020JD034163, https://doi.org/10.1029/2020jd034163, 2021.

Orth, R.: When the Land Surface Shifts Gears, AGU Advances, 2, https://doi.org/10.1029/2021AV000414, 2021.

Ossó, A., Allan, R. P., Hawkins, E., Shaffrey, L., and Maraun, D.: Emerging new climate extremes over Europe, Clim Dyn, 58, 487–501, https://doi.org/10.1007/s00382-021-05917-3, 2022.

Pastorello, G., Trotta, C., Canfora, E., Chu, H., Christianson, D., Cheah, Y.-W., Poindexter, C., Chen, J., Elbashandy, A., Humphrey, M., Isaac, P., Polidori, D., Reichstein, M., Ribeca, A., van Ingen, C., Vuichard, N., Zhang, L., Amiro, B., Ammann, C., Arain, M. A., Ardö, J., Arkebauer, T., Arndt, S. K., Arriga, N., Aubinet, M., Aurela, M., Baldocchi, D., Barr, A., Beamesderfer, E., Marchesini, L. B., Bergeron, O., Beringer, J., Bernhofer, C., Berveiller, D., Billesbach, D., Black, T. A., Blanken, P. D., Bohrer, G., Boike, J., Bolstad, P. V., Bonal, D., Bonnefond, J.-M., Bowling, D. R., Bracho, R., Brodeur, J., Brümmer, C., Buchmann, N., Burban, B., Burns, S. P., Buysse, P., Cale, P., Cavagna, M., Cellier, P., Chen, S., Chini, I., Christensen, T. R., Cleverly, J., Collalti, A., Consalvo, C., Cook, B. D., Cook, D., Coursolle, C., Cremonese, E., Curtis, P. S., D'Andrea, E., Da Rocha, H., Dai, X., Davis, K. J., Cinti, B. de, Grandcourt, A. de, Ligne, A. de, Oliveira, R. C. de, Delpierre, N., Desai, A. R., Di Bella, C. M., Di Tommasi, P., Dolman, H., Domingo, F., Dong, G., Dore, S., Duce, P., Dufrêne, E., Dunn, A., Dušek, J., Eamus, D., Eichelmann, U., ElKhidir, H. A. M., Eugster, W., Ewenz, C. M., Ewers, B., Famulari, D., Fares, S., Feigenwinter, I., Feitz, A., Fensholt, R., Filippa, G., Fischer, M., Frank, J., Galvagno, M., Gharun, M., Gianelle, D., Gielen, B., Gioli, B., Gitelson, A., Goded, I., Goeckede, M., Goldstein, A. H., Gough, C. M., Goulden, M. L., Graf, A., Griebel, A., Gruening, C., Grünwald, T., Hammerle, A., Han, S., Han, X., Hansen, B. U., Hanson, C., Hatakka, J., He, Y., Hehn, M., Heinesch, B., Hinko-Najera, N., Hörtnagl, L., Hutley, L., Ibrom, A., Ikawa, H., Jackowicz-Korczynski, M., Janouš, D., Jans, W., Jassal, R., Jiang, S., Kato, T., Khomik, M., Klatt, J., Knohl, A., Knox, S., Kobayashi, H., Koerber, G., Kolle, O., Kosugi, Y., Kotani, A., Kowalski, A., Kruijt, B., Kurbatova, J., Kutsch, W. L., Kwon, H., Launiainen, S., Laurila, T., Law, B., Leuning, R., Li, Y., Liddell, M., Limousin, J.-M., Lion, M., Liska, A. J., Lohila, A., López-Ballesteros, A., López-Blanco, E., Loubet, B., Loustau, D., Lucas-Moffat, A., Lüers, J., Ma, S., Macfarlane, C., Magliulo, V., Maier, R., Mammarella, I., Manca, G., Marcolla, B., Margolis, H. A., Marras, S., Massman, W., Mastepanov, M., Matamala, R., Matthes, J. H., Mazzenga, F., McCaughey, H., McHugh, I., McMillan, A. M. S., Merbold, L., Meyer, W., Meyers, T., Miller, S. D., Minerbi, S., Moderow, U., Monson, R. K., Montagnani, L., Moore, C. E., Moors, E., Moreaux, V., Moureaux, C., Munger, J. W., Nakai, T., Neirynck, J., Nesic, Z., Nicolini, G., Noormets, A., Northwood, M., Nosetto, M., Nouvellon, Y., Novick, K., Oechel, W., Olesen, J. E., Ourcival, J.-M., Papuga, S. A., Parmentier, F.-J., Paul-Limoges, E., Pavelka, M., Peichl, M., Pendall, E., Phillips, R. P.,

Pilegaard, K., Pirk, N., Posse, G., Powell, T., Prasse, H., Prober, S. M., Rambal, S., Rannik, Ü., Raz-Yaseef, N., Rebmann, C., Reed, D., Dios, V. R. de, Restrepo-Coupe, N., Reverter, B. R., Roland, M., Sabbatini, S., Sachs, T., Saleska, S. R., Sánchez-Cañete, E. P., Sanchez-Mejia, Z. M., Schmid, H. P., Schmidt, M., Schneider, K., Schrader, F., Schroder, I., Scott, R. L., Sedlák, P., Serrano-Ortíz, P., Shao, C., Shi, P., Shironya, I., Siebicke, L., Šigut, L., Silberstein, R., Sirca, C., Spano, D., Steinbrecher, R., Stevens, R. M., Sturtevant, C., Suyker, A., Tagesson, T., Takanashi, S., Tang, Y., Tapper, N., Thom, J., Tomassucci, M., Tuovinen, J.-P., Urbanski, S., Valentini, R., van der Molen, M., van Gorsel, E., van Huissteden, K., Varlagin, A., Verfaillie, J., Vesala, T., Vincke, C., Vitale, D., Vygodskaya, N., Walker, J. P., Walter-Shea, E., Wang, H., Weber, R., Westermann, S., Wille, C., Wofsy, S., Wohlfahrt, G., Wolf, S., Woodgate, W., Li, Y., Zampedri, R., Zhang, J., Zhou, G., Zona, D., Agarwal, D., Biraud, S., Torn, M., and Papale, D.: The FLUXNET2015 dataset and the ONEFlux processing pipeline for eddy covariance data, Scientific data, 7, 225, https://doi.org/10.1038/s41597-020-0534-3, 2020.

Prodhomme, C., Materia, S., Ardilouze, C., White, R. H., Batté, L., Guemas, V., Fragkoulidis, G., and García-Serrano, J.: Seasonal prediction of European summer heatwaves, Clim Dyn, 58, 2149–2166, https://doi.org/10.1007/s00382-021-05828-3, 2022.

Qi, Y., Chen, H., and Zhu, S.: Influence of Land–Atmosphere Coupling on Low Temperature Extremes Over Southern Eurasia, Journal of Geophysical Research: Atmospheres, 128, https://doi.org/10.1029/2022JD037252, 2023.

Rakovec, O., Samaniego, L., Hari, V., Markonis, Y., Moravec, V., Thober, S., Hanel, M., and Kumar, R.: The 2018–2020 Multi-Year Drought Sets a New Benchmark in Europe, Earth's Future, 10, https://doi.org/10.1029/2021EF002394, 2022.

Rousi, E., Fink, A. H., Andersen, L. S., Becker, F. N., Beobide-Arsuaga, G., Breil, M., Cozzi, G., Heinke, J., Jach, L., Niermann, D., Petrovic, D., Richling, A., Riebold, J., Steidl, S., Suarez-Gutierrez, L., Tradowsky, J. S., Coumou, D., Düsterhus, A., Ellsäßer, F., Fragkoulidis, G., Gliksman, D., Handorf, D., Haustein, K., Kornhuber, K., Kunstmann, H., Pinto, J. G., Warrach-Sagi, K., and Xoplaki, E.: The extremely hot and dry 2018 summer in central and northern Europe from a multi-faceted weather and climate perspective, Nat. Hazards Earth Syst. Sci., 23, 1699–1718, https://doi.org/10.5194/nhess-23-1699-2023, 2023.

Rousi, E., Kornhuber, K., Beobide-Arsuaga, G., Luo, F., and Coumou, D.: Accelerated western European heatwave trends linked to more-persistent double jets over Eurasia, Nature communications, 13, 3851, https://doi.org/10.1038/s41467-022-31432-y, 2022.

Samaniego, L., Kumar, R., and Attinger, S.: Multiscale parameter regionalization of a grid-based hydrologic model at the mesoscale, Water Resour. Res., 46, https://doi.org/10.1029/2008WR007327, 2010.

Santanello, J. A., Dirmeyer, P. A., Ferguson, C. R., Findell, K. L., Tawfik, A. B., Berg, A., Ek, M., Gentine, P., Guillod, B. P., van Heerwaarden, C., Roundy, J., and Wulfmeyer, V.: Land–Atmosphere Interactions: The LoCo Perspective, Bulletin of the American Meteorological Society, 99, 1253–1272, https://doi.org/10.1175/BAMS-D-17-0001.1, 2018.

Santanello, J. A., Peters-Lidard, C. D., and Kumar, S. V.: Diagnosing the Sensitivity of Local Land–Atmosphere Coupling via the Soil Moisture–Boundary Layer Interaction, Journal of Hydrometeorology, 12, 766–786, https://doi.org/10.1175/JHM-D-10-05014.1, 2011.

Santanello, J. A., Peters-Lidard, C. D., Kumar, S. V., Alonge, C., and Tao, W.-K.: A Modeling and Observational Framework for Diagnosing Local Land–Atmosphere Coupling on Diurnal Time Scales, Journal of Hydrometeorology, 10, 577–599, https://doi.org/10.1175/2009JHM1066.1, 2009.

Schneider, D. P., Deser, C., Fasullo, J., and Trenberth, K. E.: Climate Data Guide Spurs Discovery and Understanding, EoS Transactions, 94, 121–122, https://doi.org/10.1002/2013eo130001, 2013.

Schulzweida, U.: CDO User Guide, 2022.

Schumacher, D. L., Keune, J., Dirmeyer, P., and Miralles, D. G.: Drought self-propagation in drylands due to land-atmosphere feedbacks, Nat. Geosci., 15, 262–268, https://doi.org/10.1038/s41561-022-00912-7, 2022.

Seneviratne, S. I., Corti, T., Davin, E. L., Hirschi, M., Jaeger, E. B., Lehner, I., Orlowsky, B., and Teuling, A. J.: Investigating soil moisture–climate interactions in a changing climate: A review, Earth-Science Reviews, 99, 125–161, https://doi.org/10.1016/j.earscirev.2010.02.004, 2010.

Seneviratne, S. I., Lüthi, D., Litschi, M., and Schär, C.: Land-atmosphere coupling and climate change in Europe, Nature, 443, 205–209, https://doi.org/10.1038/nature05095, 2006.

Spensberger, C., Madonna, E., Boettcher, M., Grams, C. M., Papritz, L., Quinting, J. F., Röthlisberger, M., Sprenger, M., and Zschenderlein, P.: Dynamics of concurrent and sequential Central European and Scandinavian heatwaves, Q.J.R. Meteorol. Soc., 146, 2998–3013, https://doi.org/10.1002/qj.3822, 2020.

Stephens, G., Polcher, J., Zeng, X., van Oevelen, P., Poveda, G., Bosilovich, M., Ahn, M.-H., Balsamo, G., Duan, Q., Hegerl, G., Jakob, C., Lamptey, B., Leung, R., Piles, M., Su, Z., Dirmeyer, P., Findell, K. L., Verhoef, A., Ek, M., L'Ecuyer, T., Roca, R., Nazemi, A., Dominguez, F., Klocke, D., and Bony, S.: The First 30 Years of GEWEX, Bulletin of the American Meteorological Society, 104, E126-E157, https://doi.org/10.1175/BAMS-D-22-0061.1, 2023.

Sun, G., Hu, Z., Ma, Y., Xie, Z., Sun, F., Wang, J., and Yang, S.: Analysis of local land atmosphere coupling characteristics over Tibetan Plateau in the dry and rainy seasons using observational data and ERA5, Science of The Total Environment, 774, 145138, https://doi.org/10.1016/j.scitotenv.2021.145138, 2021.

Tawfik, A. B.: Terrestrial coupling indices, https://github.com/abtawfik/coupling-metrics/tree/master/terrestrial_coupling_index, last access: 2 November 2022, 2015.

Toreti, A., Bavera, D., Acosta Navarro, J., Cammalleri, C., Jager, A. de, Di Ciollo, C., Hrast Essenfelder, A., Maetens, W., Magni, D., Masante, D., Mazzeschi, M., Niemeyer, S., and Spinoni, J.: Drought in Europe August 2022, 2022.

Ukkola, A. M., Pitman, A. J., Donat, M. G., Kauwe, M. G. de, and Angélil, O.: Evaluating the Contribution of Land-Atmosphere Coupling to Heat Extremes in CMIP5 Models, Geophys. Res. Lett., 45, 9003–9012, https://doi.org/10.1029/2018GL079102, 2018.

van der Wiel, K., Batelaan, T. J., and Wanders, N.: Large increases of multi-year droughts in north-western Europe in a warmer climate, Clim Dyn, https://doi.org/10.1007/s00382-022-06373-3, 2022.

van Heerwaarden, C. C. and Teuling, A. J.: Disentangling the response of forest and grassland energy exchange to heatwaves under idealized land–atmosphere coupling, Biogeosciences, 11, 6159–6171, https://doi.org/10.5194/bg-11-6159-2014, 2014.

Warrach-Sagi, K., Ingwersen, J., Schwitalla, T., Troost, C., Aurbacher, J., Jach, L., Berger, T., Streck, T., and Wulfmeyer, V.: Noah-MP With the Generic Crop Growth Model Gecros in the WRF Model: Effects of Dynamic Crop Growth on Land-Atmosphere Interaction, Journal of Geophysical Research: Atmospheres, 127, https://doi.org/10.1029/2022JD036518, 2022.

Wehrli, K., Guillod, B. P., Hauser, M., Leclair, M., and Seneviratne, S. I.: Identifying Key Driving Processes of Major Recent Heat Waves, Journal of Geophysical Research: Atmospheres, 124, 11746–11765, https://doi.org/10.1029/2019JD030635, 2019.

Wei, J., Zhao, J., Chen, H., and Liang, X.-Z.: Coupling Between Land Surface Fluxes and Lifting Condensation Level: Mechanisms and Sensitivity to Model Physics Parameterizations, Journal of Geophysical Research: Atmospheres, 126, https://doi.org/10.1029/2020JD034313, 2021.

WMO: Europe has hottest summer on record: EU Copernicus, World Meteorological Organization, https://public.wmo.int/en/media/news/europe-has-hottest-summer-record-eu-copernicus, last access: 14 November 2022, 2022a.

WMO: Precipitation, relative humidity and soil moisture for July 2022, World Meteorological Organization, https://climate.copernicus.eu/precipitation-relative-humidity-and-soil-moisture-july-2022, last access: 21 February 2023, 2022b.

WMO: Precipitation, relative humidity and soil moisture for July 2018, World Meteorological Organization, https://climate.copernicus.eu/precipitation-relative-humidity-and-soil-moisture-july-2018, last access: 21 February 2023, 2018.

WMO: WMO Guidelines on the Calculation of Climate Normals: Tech. Rep. WMO-No. 1203, World Meteorological Organization, 2017.

WMO: 2015 second hottest year on record for Europe, World Meteorological Organization, https://public.wmo.int/en/media/news/2015-second-hottest-year-record-europe, last access: 27 October 2022, 2015.

WMO: WMO STATEMENT ON THE STATUS OF THE GLOBAL CLIMATE IN 2003: Tech. Rep. WMO-No. 966, World Meteorological Organization, 2004.

Xoplaki, E., Ellsäßer, F., Grieger, J., Nissen, K. M., Pinto, J., Augenstein, M., Chen, T.-C., Feldmann, H., Friederichs, P., Gliksman, D., Goulier, L., Haustein, K., Heinke, J., Jach, L., Knutzen, F., Kollet, S., Luterbacher, J., Luther, N., Mohr, S., Mudersbach, C., Müller, C., Rousi, E., Simon, F., Suarez-Gutierrez, L., Szemkus, S., Vallejo-Bernal, S. M., Vlachopoulos, O., and Wolf, F.: Compound events in Germany in 2018: drivers and case studies, 2023.

Yin, X. and van Laar, H. H.: Crop systems dynamics, https://models.pps.wur.nl/gecros-detailed-eco-physiological-crop-growth-simulation-model-analyse-genotype-environment, last access: 1 March 2023, 2005.

Yin, Z., Findell, K. L., Dirmeyer, P., Shevliakova, E., Malyshev, S., Ghannam, K., Raoult, N., and Tan, Z.: Daytime-only mean data enhance understanding of land–atmosphere coupling, Hydrol. Earth Syst. Sci., 27, 861–872, https://doi.org/10.5194/hess-27-861-2023, 2023.

Zink, M., Samaniego, L., Kumar, R., Thober, S., Mai, J., Schäfer, D., and Marx, A.: The German drought monitor, Environ. Res. Lett., 11, 74002, https://doi.org/10.1088/1748-9326/11/7/074002, 2016.